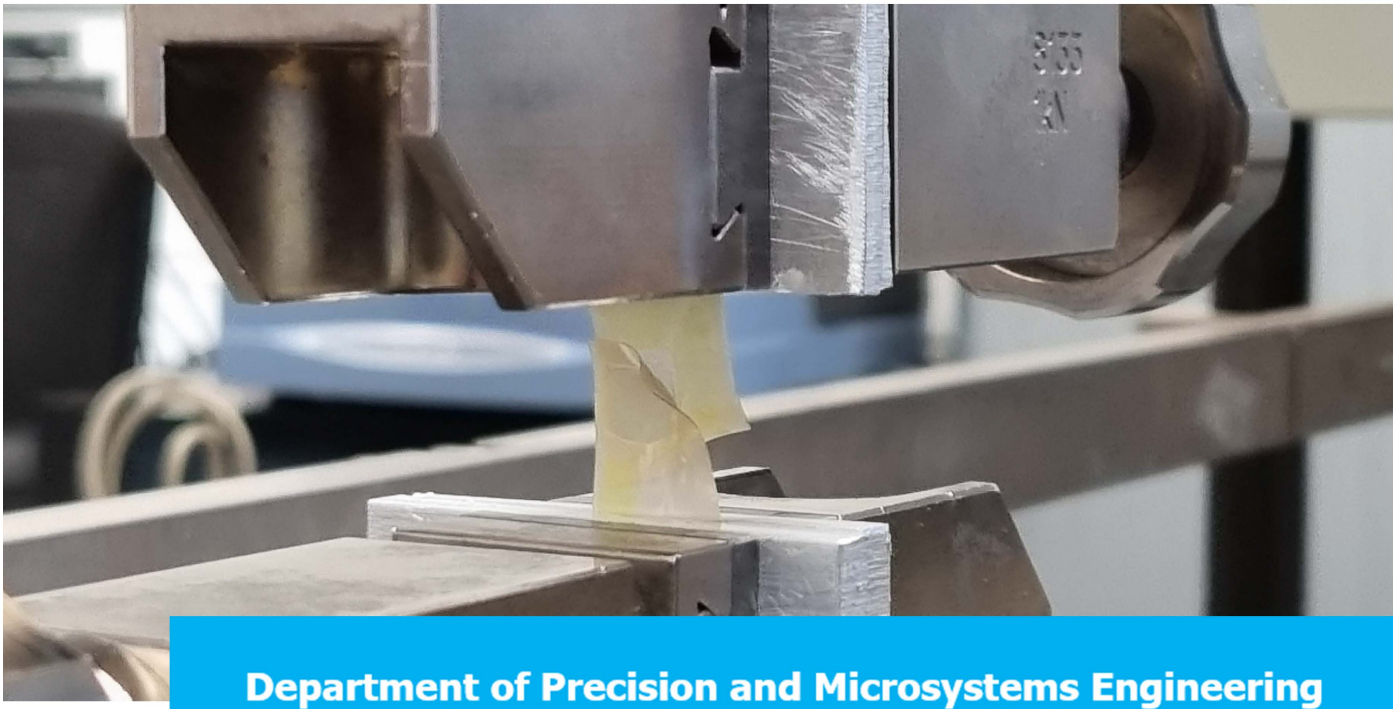

Department of Precision and Microsystems Engineering

Laser Transmission Welding of thin PEEK films

Ward Dijkman

Report no	:	**2024.042**
Coach	:	Dr.ir. Marcel Tichem
Professor	:	Dr.ir. Marcel Tichem
Specialisation	:	Micro & Nano Engineering
Type of report	:	Master thesis
Date	:	11 July 2024

Laser Transmission Welding of thin PEEK films

by

Ward Dijkman

Supervisors: Dr. Ir. M. Tichem, H.M. Bilyalova MSc and F.M. Conte Capodacqua MSc
Faculty: Mechanical Engineering (ME)

TU Delft

Acknowledgements

First, I would like to express my gratitude to everyone involved in the MECOMOS project for their invaluable advice during our monthly meetings, and especially to Mareen for supplying the 3D thermoformed samples crucial for this report. Special thanks go out to my supervisors: Hava, for her insights into PEEK and its material properties; Filippo, for his explanations on the physics of laser and polymer interactions, as well as his practical tips for laser welding of polymers; and Marcel, for his guidance throughout my research and his help in maintaining a clear overview of the process as we developed a new procedure for laser transmission welding.

Furthermore, I thank Dr.-Ing. Rolf Klein and the support team at Clearweld for their guidance in choosing the right absorption coating and for instructing me on how to apply the coating optimally.

In addition, my gratitude extends to the lab technicians who were instrumental during my research. I thank Gideon for his assistance with the laser setup, Patrick for his help in performing the tensile tests, and Alex for his support in the chemical lab and cleanroom.

Lastly, I would like to acknowledge the support of my friends and family, who backed me throughout my entire study process in Delft. Their support and encouragement have been a constant source of motivation.

Ward Dijkman
Delft, July 2024

Summary

For the design of new manufacturing methods for mechanical metamaterials in compact motion systems, a new bonding technique has been developed. The manufacturing technique requires thermoformed PEEK films to be bonded together. Literature review has shown that laser welding, and specifically laser transmission welding, is a valuable method for this manufacturing technique, particularly for bonding materials that are tens of microns thick, such as thermoformed and PEEK films. This research demonstrates how to define a viable process and how to optimize laser parameters to achieve maximum joint strength and identifies factors that can diminish the quality of the bond, thereby affecting optimal speed.

Further investigation of the PEEK and absorptive coating spectral curves has revealed that absorption coating is effective in increasing the absorbance used in this research. Welding with an infrared laser around one µm wavelength can rapidly produce strong welds, where the tensile strength of the welds exceeds that of the material. A fluence of around 20 to 30 mJ/mm^2 results in optimal weld peel strengths.

The optimal parameters for 125 µm lap welding include a speed between 10 and 15 millimeters per second and a defocussing distance between 4 and 7 millimeters. The thickness of the welded films range from 25 to 125 microns. It has also been observed that thicknesses of 25 and 50 micrometers can produce welds with 125 thick thermoformed PEEK films, allowing for 2.5D film welding capabilities.

Contents

Acknowledgements i

Summary ii

1 Introduction 1
- 1.1 Mechanical Metamaterials . . . 1
  - 1.1.1 MECOMOS . . . 1
- 1.2 Microjoining . . . 2
- 1.3 Motivation . . . 2
  - 1.3.1 Research objective . . . 3
- 1.4 Report outline . . . 4

2 Laser welding of polymers 5
- 2.1 Laser welding . . . 5
  - 2.1.1 Laser Transmission Welding (LTW) . . . 5
  - 2.1.2 Laser parameters . . . 6
- 2.2 Polymers . . . 8
  - 2.2.1 PEEK . . . 9
  - 2.2.2 Crystallinity . . . 9
  - 2.2.3 Welding failure modes . . . 9
- 2.3 Laser welding of polymers . . . 10

3 Methodology 12
- 3.1 Material . . . 12
  - 3.1.1 PEEK film . . . 12
  - 3.1.2 Clearweld absorptive coating . . . 12
- 3.2 Equipment . . . 13
  - 3.2.1 Spectrometer . . . 13
  - 3.2.2 Lasea laser . . . 13
  - 3.2.3 Clamping device . . . 14
  - 3.2.4 Peel force tester . . . 15
  - 3.2.5 Tensile tester . . . 15
  - 3.2.6 Oven . . . 15
  - 3.2.7 Microscopes . . . 15
- 3.3 Testing methods . . . 15
  - 3.3.1 Welding process . . . 15
  - 3.3.2 Thermal treatment test . . . 16
  - 3.3.3 Data analysis . . . 16

4 Results 17
- 4.1 Spectral properties PEEK and Clearweld . . . 17
- 4.2 Thermal treatment . . . 19
  - 4.2.1 Stress strain relationship . . . 19
  - 4.2.2 Optical properties . . . 20
  - 4.2.3 Roughness . . . 20
- 4.3 Welding . . . 21
  - 4.3.1 Post-weld pictures . . . 21
- 4.4 Peel tests . . . 22
- 4.5 Laser parameters . . . 23
  - 4.5.1 Fluence calculations . . . 23
  - 4.5.2 Laser speed . . . 24

4.6 Defocussing distance 24
4.7 Weld shape 26
4.7.1 Pitch distance 26
4.7.2 Hatch pattern 28
4.8 Welding different thicknesses 28
4.9 Welding thermoformed sheets 29

5 Discussion & Conclusion **30**
5.1 Discussion 30
5.2 Conclusion 30
5.3 Recommendations and future work 31

References **32**

A Appendix A - LTW step by step guide **33**
A.1 Laser parameters 35

1 Introduction

This chapter introduces the MECOMOS project, provides a brief summary of related literature on microjoining methods, outlines the motivation for this research, and presents the problem statement and report outline.

1.1. Mechanical Metamaterials

A metamaterial is a material that possesses unique characteristics due to a structured micro-architecture. This makes it possible to integrate different qualities and functions, creating new challenges in the development, production, and characterisation of functional components. Applications for mechanical metamaterials include vibration damping devices, lightweight construction, and outstanding precision capabilities. One other way to manufacture mechanical metamaterials is by stacking and joining layers of thermoformed layers on top of each other. The joining of thin unsupported foils could pose challenges. [12]

1.1.1. MECOMOS

Mechanical metamaterials could be manufactured by assembly, additive, and subtractive manufacturing. Most mechanical metamaterials in research are manufactured by additive manufacturing. . The project will focus on designing and researching a promising joining concept for the fabrication of mechanical metamaterials at the microscale. This TU Delft project (called MECOMOS) is researching and developing a mechanical metamaterial compact motion system and a concept is shown in figure 1.1.

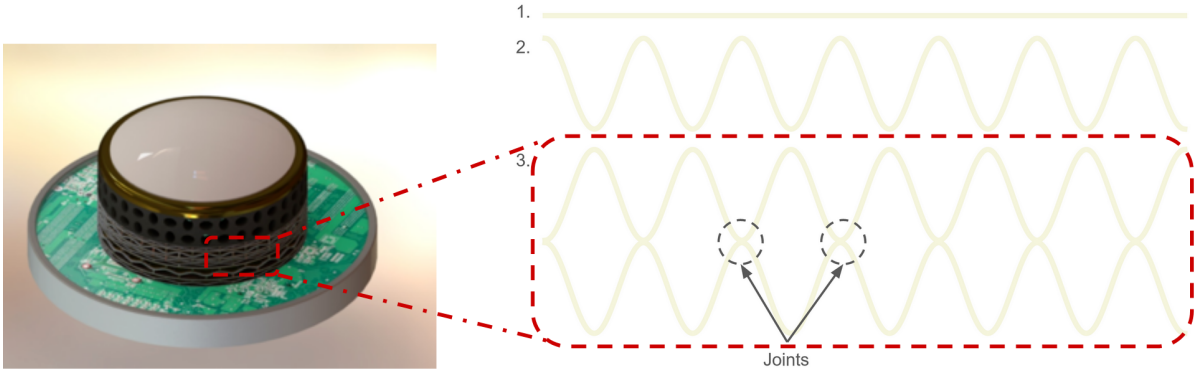

Figure 1.1: On the left is the MECOMOS concept of a mechanical metamaterial compact motion system [15] and on the right the MECOMOS manufacturing steps are shown with 1. the initial flat PEEK sheet, 2. the thermoformed sheet, and 3. the joined sheets

1.2. Microjoining

Joining is one of the fundamental manufacturing techniques, and the technique allows the manufacturing of more complex and multi-material products. Joining methods are crucial in many industries, as they allow for the creation of high-quality, reliable, and functional products. Currently, a lot of research and development is in stacking multiple chips on top of each other to increase performance. In applications where a smaller feature size increases performance, novel methods of manufacturing are required.Furthermore, innovative joining methods at the microscale open up new areas to be researched and developed. Examples of these products are stents to treat blood cloths, in-ear hearing aids, and batteries. [5]

1.3. Motivation

Currently, most of the mechanical metamaterials in research are manufactured using additive manufacturing techniques. Mechanical metamaterials could be manufactured by assembly, additive, and subtractive manufacturing. Additive manufacturing for metamaterials is not scalable as a result of the slow nature of additive manufacturing. For subtractive manufacturing, the complication lies in the difficulty of removing material inside the workpiece to manufacture the intricate features that metamaterials often have. The assembly and joining, as the object would not stay assembled if not joined, process generally requires more effort and time to finally finish the metamaterial. The project will focus on designing and proofing a joining concept for the fabrication of mechanical metamaterials on the microscale.

Previously, a literature study (see figure 1.2) was conducted to investigate possible solutions to the challenge mentioned in the previous paragraph. This research advised three possible joining techniques: laser welding, autohesion, and thermoplastic adhesive bonding. Laser welding was chosen to investigate this technique further. The reason for this choice is the versatility with respect to joining different materials, different geometries, different thicknesses, and different bond geometries. In addition, the process is fast and requires minimal pretreatment and posttreatment.

With joining at the microscale with high throughput comes different challenges and implications. An implication is achieving sufficient positioning precision with the joining method, matching the architectural details of the metamaterial. Besides precision, the resolution of the joining method is also crucial. The resolution refers to the minimum area that a joint could achieve for a certain joining method. The resolution could be affected by the diameter of the tip in spot welding, the cross section at the laser focal point for laser welding, the diameter of a droplet of adhesive, or the contact area of an ultrasonic welding tool. Furthermore, the metamaterial should handle the applied force which is required for certain joining methods, such as solid-phase welding.

There are still hurdles to overcome to validate the laser joining process as a fruitful joining method in the MECOMOS project. The purpose of this project is to manufacture intricate mechanical metamaterials by thermoforming PEEK films, then stacking and joining the films.

Literature research ([7]) has shown the potential of laser welding as a method of joining 2.5D thermoformed polymer sheets to construct compact motion systems consisting of mechanical metamaterials. In figure 1.2 an overview of microjoining methods is presented. Laser welding offers very fast joining times, can achieve tensile and shear strength equal to or greater than the base material, and requires only minimal clamping pressure. The spot size of lasers can be narrowed down to a few micrometers, and the laser parameters can be precisely controlled. This makes laser welding a versatile method, with the added advantage of effectively joining dissimilar materials at high speeds compared to other methods.

To determine if the promising joining method, laser welding, is fit for the project, several subquestions have to be answered. First, the process of welding relatively thick PEEK films (125 µm) as done in the paper by Amanat et al. [2] must be recreated with a thinner PEEK film with equipment from the Precision and Microsystems Engineering lab of TU Delft.

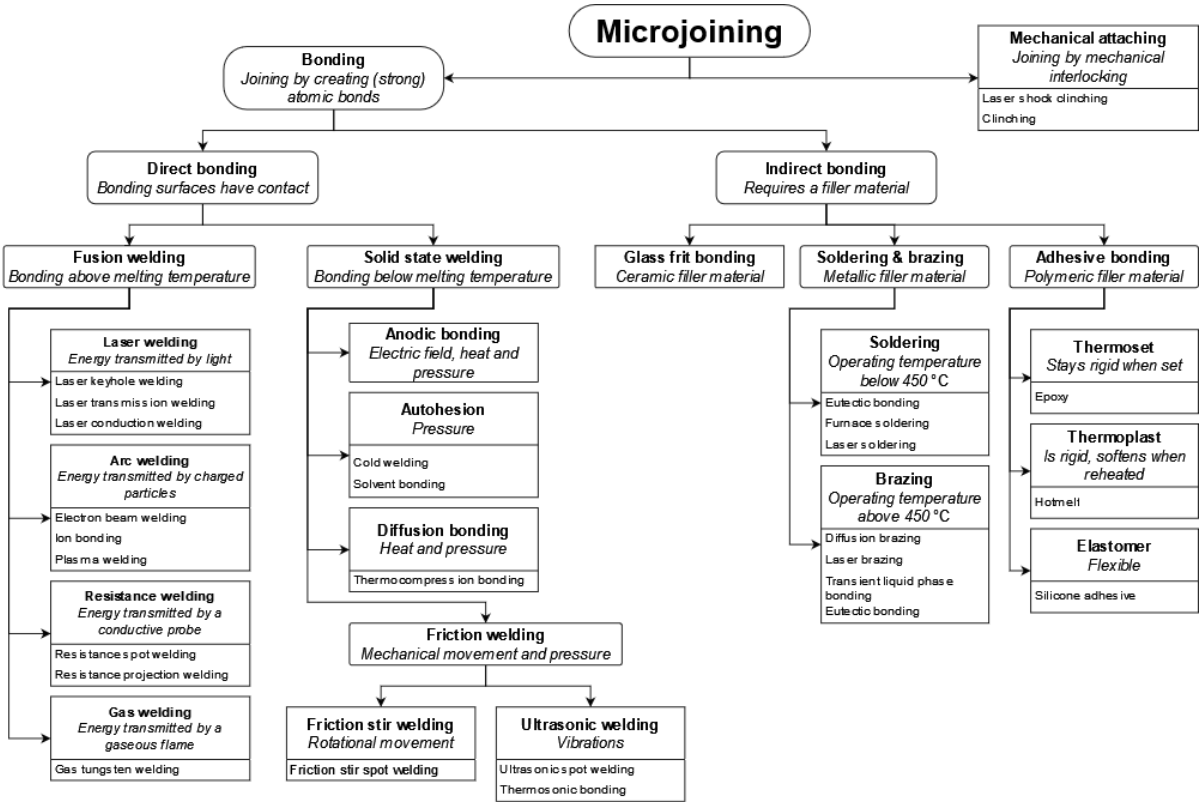

Figure 1.2: Overview of microjoining methods (from [7])

Finally, process parameters such as laser power, welding speed, clamping pressure, irradiation time, laser beam size and depth, and additives (like absorbing coatings) will be optimized to achieve higher peel strengths.

1.3.1. Research objective

The main research question will be: What effect do different laser process parameters, such as speed, defocussing distance, and geometry of the lasers' path have on peel strength of lap welded PEEK films? Next to the main research question, the following sub-questions will be investigated:

- Which set of parameters, e.g. laser speed, fluence, pitch size, etc., allow for the highest peel strength for welding 125 µm thick PEEK films?
- Can laser transmission welding be applied to create joints in 3D structures made from thermoformed PEEK films?
- What is the influence of a laser on the material properties of PEEK?

The research will contribute to knowledge by improving the process of joining mechanical metamaterials with a microscale feature size.

1.4. Report outline

In the next chapter 2 (Laser welding of polymers), the topics of laser welding, polymers, and the laser transmission welding of PEEK will be covered. In chapter 3 (Methodology), the materials and equipment used will be explained, as well as the welding and testing process. The penultimate chapter 4 (Results) will present the results of the research. Finally, in chapter 5 (Discussion & Conclusion) the results will be discussed, the conclusion and possible future work will be shown.

2

Laser welding of polymers

In this section, the theoretical background of this research will be given. First, a look will be taken into laser welding and laser physics. Thereafter, the workings of polymers, especially PEEK, will be explained.

2.1. Laser welding

Lasers, abbreviation for Light Amplification by Stimulated Emission of Radiation, are devices that emit light through a process of optical amplification. They produce highly coherent and monochromatic beams of light, which can be precisely focused to achieve high energy densities. Laser welding is a technique that utilizes the intense energy of a laser beam to join materials together. The high precision and control offered by lasers allow for the welding of intricate and delicate components with minimal heat distortion. This process is particularly advantageous for materials that are difficult to weld using conventional methods, such as polymers and high-strength alloys, providing strong and durable welds with high efficiency.

2.1.1. Laser Transmission Welding (LTW)

Figure 2.1 provides an overview of the laser transmission welding setup used for lap joints in this research. Various parameters and materials are depicted in this figure. From left to right, the nearest component is an arrow labelled F, indicating one of two forces pressing down on the transparent blue glass. This force applies pressure to the peak film while allowing laser light to pass through, as the glass is transparent. Next, a green Clearweld coating is placed at the interface between two PEEK films, which are shown to lie on top of each other. Following this, the laser beam shown in red moves with a velocity denoted as V in the direction of the arrow. The focal point of the beam is depicted as the narrowest part of the red line. The distance between this focal point and the interface of the two films, where the clear weld coating is located, is referred to as the defocussing distance (L_d). In summary, this setup represents the essential elements of laser transmission welding.

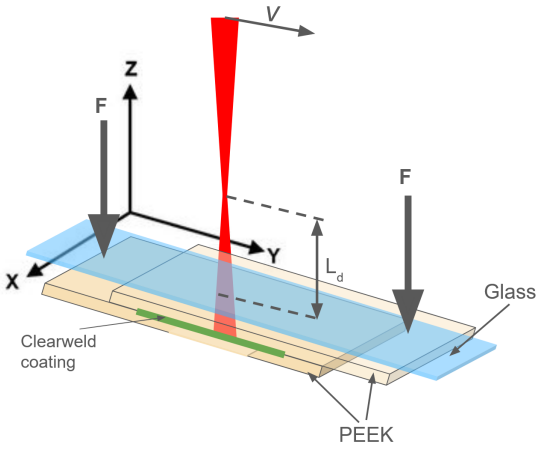

Figure 2.1: Overview of the LTW process, with V laser writing speed, L_d the defocussing distance, and F the clamping force

2.1.2. Laser parameters

There are several dependent and independent parameters that influence the existence of a weld, its strength, and its eventual outcome. For this research, it is primarily possible to analyse independent variables in relation to each other, although this is not always feasible. In addition, the research will examine the influence of dependent parameters, with particular emphasis on fluence as the main factor. Fluence encompasses various laser parameters that can be manipulated through laser setup, and these parameters are interrelated. To increase fluence, one can increase pulse energy, burst rate, and pulse rate, while decreasing speed, burst time, and defocussing distance. As illustrated in figure 2.2, pulse energy refers to the energy contained in a single pulse. Speed, in this context, refers to the velocity at which the laser beam moves relative to the sample. [9]

Independent

- Clamping pressure [MPa]
- Thickness PEEK [µm]
- Fluence [J/cm^2]
- Height of Clearweld coating [nm]

Dependent (Fluence$\uparrow$ $\Phi = E/A$ [J/mm^2])

- Pulse energy [µJ] $\uparrow$
- Speed [mm/s] $\downarrow$
- Burst Time [µs] $\downarrow$
- Burst Rate [Hz] $\uparrow$
- Pulse Rate [Hz] $\uparrow$
- Defocussing distance [mm] $\downarrow$

Fluence

The fluence is the energy per unit area that a laser deposits into a material. Fluence is typically dependent on several parameters, including pulse energy, speed, burst time, burst rate, pulse rate, and defocussing distance. Generally, fluence is expressed in joules per square millimeter (J/mm^2). Fluence is an important parameter because it determines whether the amount of energy delivered to the welding material is adequate. Too much fluence can lead to excessive energy input, causing damage to the material, while too little can result in insufficient energy for effective welding. [18]

Pulses

The femtosecond laser utilizes pulses to transfer energy to the material. The rate of pulses, the number of pulses in a burst, and the burst rate are all parameters that can be adjusted to control the energy delivery. These parameters are illustrated in figure 2.2, where the interplay of these factors can be observed.

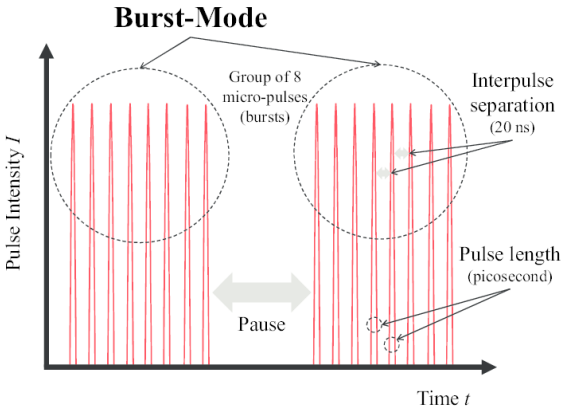

Figure 2.2: Pulse and burst rates (from [8])

Laser beam profile

The laser beam profile can be calculated with its beam quality factor (M^2), the wavelength and the beam waist radius. The beam quality factor indicates how close the beam is to an ideal Gaussian beam distribution. Next to the beam quality factor, the wavelength (λ) and the beam waist radius (w_0) at the smallest spot size, also called the focal point, determine the Rayleigh range (z_r) in equation 2.2. [17]

$$w(z) = w_0 \sqrt{1 + \left(\frac{z}{z_r}\right)^2} \tag{2.1}$$

$$z_r = \frac{\pi w_0^2}{M^2 \lambda} \tag{2.2}$$

Implementing 2.2 in equation 2.1 results in equation 2.3, which can be used to determine the spot size of different distances from the focal point. The results of the equation 2.3 with different M^2 values is plotted in figure 2.3 b.

$$w(z)^2 = w_0^2 \left[1 + \left(\frac{z - z_0}{z_r}\right)^2 \left(\frac{M^2 \lambda^2}{\pi w_0^2}\right)^2\right] \tag{2.3}$$

The beam waist is given by the manufacturer but changes due to the lens. The area from the laser is larger than that seen in PEEK. The Clearweld is another different indicator. As can be seen in figure 2.3 a, at certain defocussing distances away from the focal zero point the power density spread more evenly, thus providing less differentiation in fluence and thus improving weld quality. The energy density in the figure is more spread compared to the laser used in this research because of the higher M^2 factor.

In figure 2.4, the Gaussian curves of the laser are depicted, alongside the thresholds of the polymeric material. Different colors in the figure illustrate various ways the intensity or energy of the laser interacts with or alters the polymer. If the laser intensity remains below the welding threshold, the polymer is merely heated, and no significant changes occur. However, if the laser intensity exceeds the welding threshold, indicated in green, the PEEK film of the polymer is welded together. Further exceeding the burning threshold results in burning of the material.

The figure demonstrates that three distinct effects can occur at the laser's focal point: heating, welding, and burning. The optimal welding condition is achieved when the laser intensity falls below the

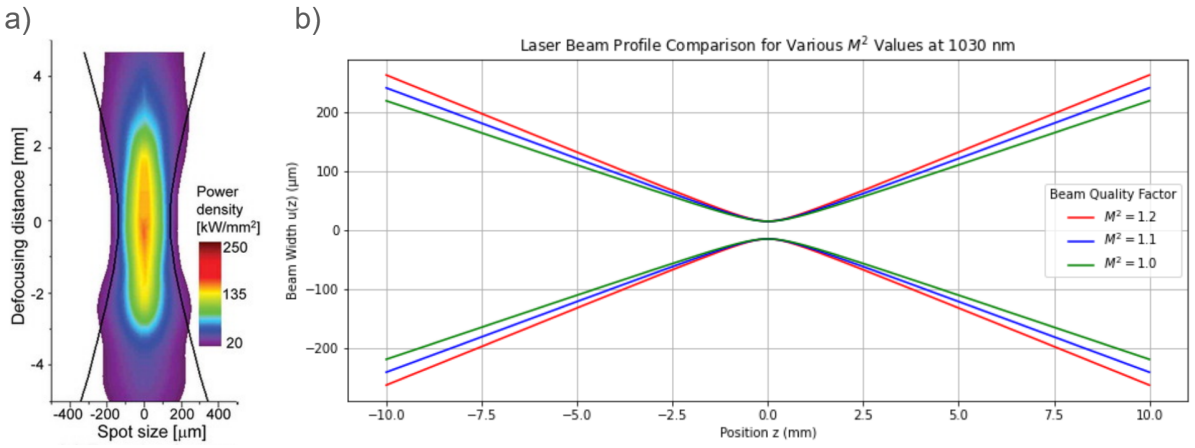

Figure 2.3: a) Power density of a (16 kW, 1030 nm, M^2 = 24) laser (from [10]) and b) laser beam profile of a 1030 nm laser with a waist size of 30 µm

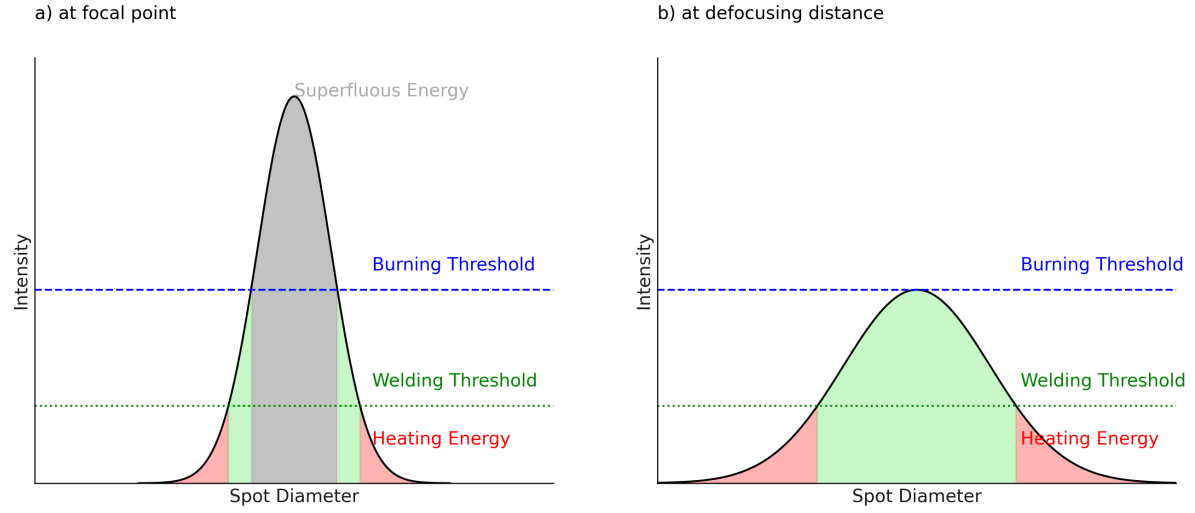

Figure 2.4: Gaussian curves of the laser beam with the burning and welding thresholds of a beam a) at the focal point and b) at a defocussing distance. In red a heated, in green a welded and in gray burned spot diameters of PEEK are schematically shown

burning threshold yet remains above the welding threshold. Identifying this precise range of laser intensity is a challenging task.

2.2. Polymers

Polymers, derived from the Greek word ”πολυμερής” meaning ”having many parts”, are materials made up of long chains of repeating units called monomers. Unlike metals or ceramics, polymers exhibit unique characteristics depending on the temperature and the rate of deformation applied to them [13]. Thermoplastics, elastomers, and thermosetting polymers are three types of plastics with different characteristics. Thermoplastics, like the plastic used in water bottles, can be heated and reshaped multiple times, which makes them easy to recycle. Elastomers are very stretchy and flexible, like rubber in tyres or elastic bands, and can go back to their original shape after being stretched. Thermosetting polymers are the opposite of thermoplastics because once they are heated and set, they cannot be melted or reshaped. They are really tough and are used in applications like car parts and electrical components because they can handle a lot of heat and stress. [20]

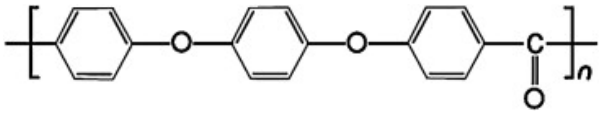

Figure 2.5: Chemical structure of PEEK (from [13])

2.2.1. PEEK

Polyetheretherketone (PEEK) is classified as a material with high strength, high toughness, high heat resistance, excellent thermal conductivity, low shrinkage, good dimensional stability, and good flammability performance. The monumeric part of PEEK is shown in figure 2.5. PEEK is a thermoplastic and thus can be processed by heating to give it a new form or join two separate PEEK parts together. An important distinguishing feature of polymers is how their properties change with temperature. Typically, when heated, many polymers experience three primary thermal transitions: the glass transition temperature (Tg), the melt temperature (Tm), and the flow temperature (Tf). Additionally, PEEK components exhibit a fourth transition, known as the recrystallization transition (Tc), which depends on their initial fabrication process. [3] & [13]

2.2.2. Crystallinity

Crystallinity in polymers, particularly thermoplastics, refers to the degree to which polymer chains are organized into a highly ordered, repeating structure known as a crystalline lattice. Unlike amorphous polymers, which have randomly coiled and entangled molecular chains, crystalline polymers have regions where the chains are aligned and packed in a regular pattern. There is also a mix between those two, semi-crystalline as can be seen in figure 2.7. The degree of crystallinity can significantly influence the physical properties of a polymer. Higher crystallinity typically enhances stiffness, tensile strength, and resistance to solvents and heat, while reducing flexibility and transmissibility. [19]

The crystallisation process in polymers affects the thermal history of the material. During cooling from the molten state, polymer chains can form crystalline regions or remain in an amorphous state, depending on the conditions. Annealing, or heating the polymer above its glass transition temperature but below its melting temperature, can increase crystallinity by allowing chains to rearrange into a more ordered structure. This process can enhance the material's performance characteristics but can also lead to increased brittleness and decreased transparency due to light scattering from the crystalline regions. [1]

Optical properties

The total incident light, or radiation, is the sum of direct transmitted light, absorbed radiation, internal reflection, and direct reflected light, and these components should together account for 100 % of the incident energy. In figure 2.8 this is shown. As the thickness of a material increases, its transmissibility decreases, while absorption increases. The type of material and, in particular, its surface properties determine the percentage of reflection. The arrangement of molecules, particularly in polymers, significantly influences internal absorption or dispersion. [11]

In more crystalline polymers, the polymer chains are tightly packed, making it harder for light to pass through. Consequently, the density of the polymer increases, transmissibility decreases, and the material becomes more opaque. For example, an amorphous form of PEEK is transparent, whereas a semi-crystalline PEEK with low crystallinity appears translucent and has a beige colour. [19]

2.2.3. Welding failure modes

There are different types of failure modes of polymeric welds, as illustrated in figure 2.6. One such mode occurs when the bond breaks at the weld, indicating that the substrate strength, or the material strength, exceeds the bond strength. Another mode occurs when the substrate itself breaks, suggesting that the bond is stronger. This is common in conventional welding, where the presence of more material and a good weld ensure that the two parts welded together form a singular entity. This type of substrate failure is categorized as a type I failure. A type II substrate failure involves breaking near the interface. There is also a mixed type substrate failure, where the break occurs partially within the substrate and

partially within the weld, as well as a mixed type II failure, which occurs mostly at the interface, but also involves some of the substrate. These failure modes are particularly useful in the later stages of testing to evaluate the quality of the weld. Ideally, a laser weld would result in substrate failure, indicating that the weld has successfully created a uniform, singular material. [2]

Mechanism	Description	Appearance	Inference	Details
Interfacial	Interfacial failure		Bond strength≪substrate strength	Interfacial failure at bond. Most undesired result.
Substrate (Type I)	Bulk substrate failure		Bond strength≫substrate strength	Substrate results in tensile yield and break. This implies that the joint is as strong as possible, where the substrate will fail first. Most desired result.
Substrate (Type II)	Near interfacial substrate failure		Bond strength>substrate strength	Failure within the substrate, but near the interracial region and bond still intact.
Mixed (Type I)	Substrate and interfacial		Bond strength~substrate strength	Failure partially within substrate and at the bond interface.
Mixed (Type II)	Interfacial and some substrate		Bond strength<substrate strength	Failure mostly interfacial. but with some substrate failure, e.g. in the form of plastic deformation.

Figure 2.6: Different kind of failure modes (from [2])

2.3. Laser welding of polymers

The welding process is achieved by heating the film until it melts and then applying the right amount of pressure to ensure that the molten polymer surface adheres closely to the substrate.

The light from near-infrared lasers, such as the one used in this experiment, interacts with polymeric materials by stimulating the oscillation of electrons. These oscillations lead to an increase in temperature, which causes the polymer chains to flow together and encourages the formation of secondary valence bonds between the atoms in the chains, resulting in interchain links. In addition to light absorption, radiation intensity loss in polymeric materials can also occur due to scattering caused by the material's internal structures. The scattering of radiation in polymeric materials is influenced by the microscopic structure of the material, such as crystallites, amorphous regions, or inclusions. These structural inhomogeneities lead to the dispersion of light, which can reduce the efficiency of light transmission and contribute to the overall loss of radiation intensity within the material. This scattering effect is denoted by the symbol S in figure 2.8. To increase temperature by heat conduction, the joint interfaces of the components must be tightly and parallelly fixed using appropriate clamping devices. Additionally, the surface roughness of the joint interface should be minimized to enhance thermal contact efficiency. [14] & [4]

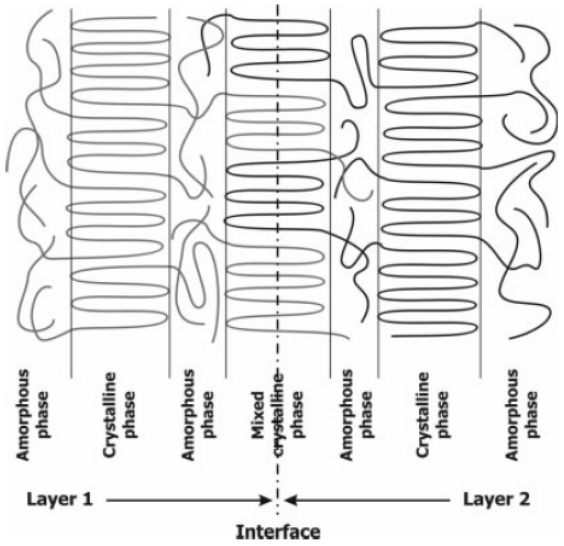

Figure 2.7: The entangling of semicrystalline polymers (from [11])

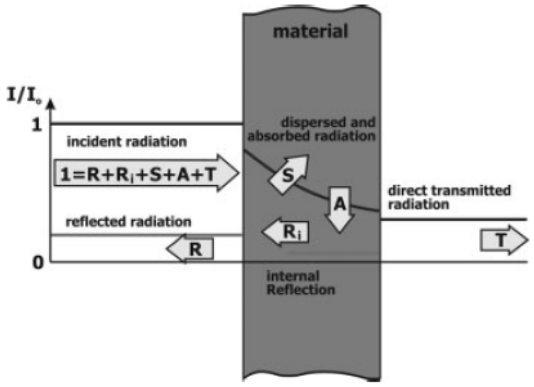

Figure 2.8: Drawing of the reflective, transmissive and absorptive paths light takes when interacting with a material (from [11])

3 Methodology

In this chapter the project and the machines and processes used to perform and analyse the welds will be discussed.

3.1. Material

In this section, the material properties of PEEK as well as how the samples were cut will also be discussed. Furthermore, the specifications of the absorptive coating will be given.

3.1.1. PEEK film

The Aptiv series PEEK from Victrex is used in this research. The specifications of the PEEK films are shown in table 3.1. The difference in thickness influences Young's modulus and the tensile stress. The variation in those values within a certain thickness is due to the higher value measured with respect to the machine direction and the lower value in the transverse direction. As the PEEK was supplied in sheets and not in rolls, it could not be determined which direction was transversal and which was machine. Therefore, the average of those two will be used in the report. The PEEK films have a rough, grainy side and smooth side.

Samples

The PEEK sheets were cut with a paper roller cutter into samples of 2 by 3 centimetres with a deviation of $\pm$ 1 mm. For this research three different kinds of PEEK thicknesses were used, 25, 50 and 125 µm. The 125 µm thickness is used as the standard thickness, except for the experiments comparing the effect of different thicknesses on weld quality. When in this report no thickness of the PEEK film is mentioned, the report refers to the 125 µm films.

3.1.2. Clearweld absorptive coating

The only additional material used to weld PEEK in this research is the absorptive coating, Clearweld LD 920J [6]. The coating is acetone based and has to be applied to both surfaces at the weld interface. The manufacturer doesn't disclose any information about the content of the coating. The Clearweld coating is intended for wavelengths between 940 and 1100 nm. The coating will be applied with a marker. The recommended setting is 60-120 nl/mm^2 and acetone evaporates in roughly 10 seconds. Before coating could be applied, the samples have to be cleaned with isopropanol to remove grease and dust from the surface. The cleaning and coating will be done in a fume hood to ensure a dry environment and to protect the operator from inhaling toxic acetone gasses. The application will also be done in a low dust environment to prevent dust particles on settling on the surface. Dried Clearweld laser welding coatings are sensitive to UV light, sunlight, high storage temperatures, and various chemicals. To limit exposure to these conditions, the coated samples will be stored in closed containers and prepared shortly before welding. The Clearweld is applied to the smooth, glossy side of the PEEK. There are several reasons for the side of absorptive coating, two flat surfaces have more contact points, thus aiding with a better weld. Furthermore, is it easier to apply an uniform coating to an even surface.

Table 3.1: Specifications of Aptiv 1000 series PEEK films with thicknesses of 25, 50 and 125 µm. All values at 23°C unless specified otherwise [3]

	Value	Unit
Density	1.30	g/cm^3
Melting point	343	°C
Glass transition temperature	143	°C
Shrinkage at 200 °C	< 2	%
Tensile elongation	> 150	%
	Young's moduli	
25 µm	2.6 - 2.8	GPa
50 µm	2.5	GPa
125 µm	2.3 - 2.4	GPa
	Tensile stresses	
25 µm	120 - 140	MPa
50 µm	120 - 130	MPa
125 µm	120	MPa

Table 3.2: Pharos laser source specifications

	Value	Unit
Maximum pulse energy	200	µJ
Pulse duration	290-10,000	fs
Beam quality (M^2)	≤ 1.2	–
Beam waist radius	15	µm
Repetition rate	1-1000	kHz
Type laser	Yb solid state	–
Wavelength	1028 (±5)	nm

3.2. Equipment

In this section the equipment used for the project will be discussed.

3.2.1. Spectrometer

The AvaSpec NIR-256 spectrometer was used in combination with the AvaLight DH-S-BAL. The AvaSpec covers a range of wavelength from 900 to 1750 nm with a resolution of 4 nm. The reflectance and transmittance will be measured and the absorption will be determined using those two measurements.

3.2.2. Lasea laser

The Lasea micromachining station (see Figure 3.2 a) is a laser system composed of the Pharos Ph1 laser source, the LS-lab setup, LS-beam management system, LS-scan head, LS-view vision module and the Aerotech XY stage and the telecentric Linos Ronar F-theta IR lens.

Laser parameters

To distinguish the effect different parameters have on the ability and quality of the weld, the parameters and the weld environment are kept equal. With the Lasea laser the following parameters can set, the speed (mm/s), the jump speed (mm/s), the pulse rate (Hz), the pulse width (µs), the power (%), the burst time (µs), the repetition rate (kHz), and the burst rate (Hz).

Pharos laser source

The Pharos has a beam quality factor of 1.2 or less, indicating an almost ideal Gaussian beam profile. The beam profile can be seen in figure 3.1 b. The Pharos is a femtosecond, solid state pulsed laser and its fundamental wavelength is 1030 nm. It has a maximum output power of 15 W and the other specification can be seen in table 3.2.

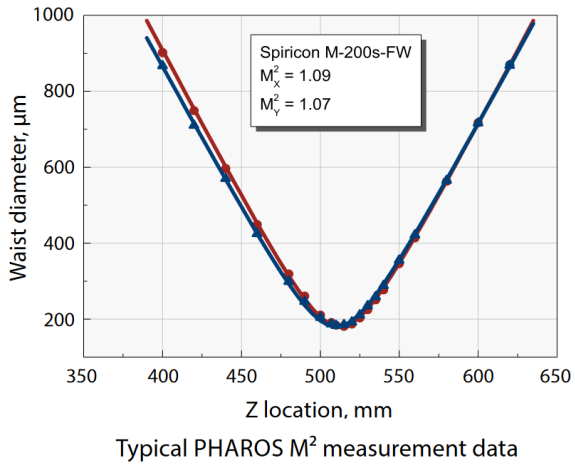

Figure 3.1: The waist diameter and M^2 values of the Pharos laser source [16]

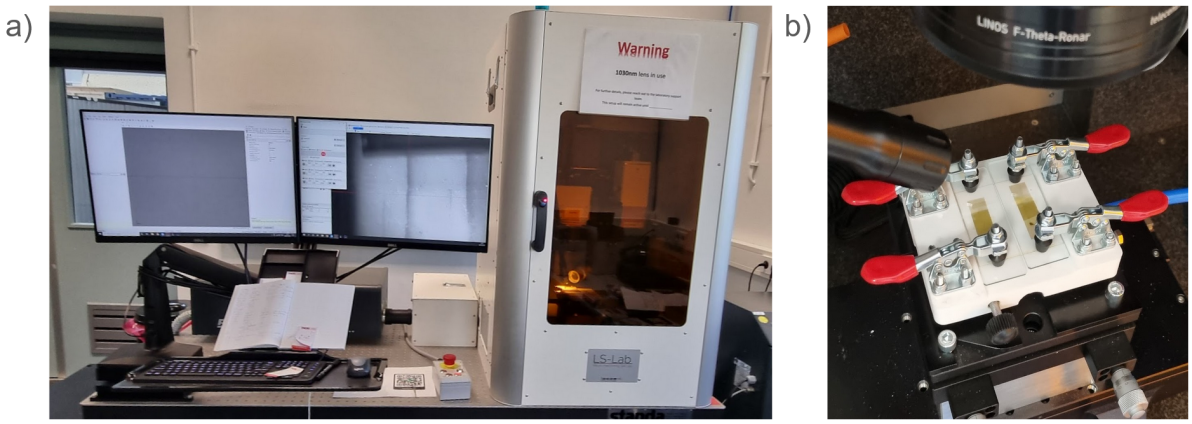

Figure 3.2: Laser welding setup with a) the Lasea laser and b) clamping device with PEEK samples

3.2.3. Clamping device

The clamping device (see figure 3.2 b) consists of a frame, two set screws, four toggle clamps, an alumina plate and two microscopy glasses. The 3D printed (PLA) frame is used to keep all the parts together. The set screws allows the clamping device to be swiftly and easily attached and detached to the Lasea XY stage. The alumina plate provides a flat, smooth surface on which the PEEK samples are laid. Furthermore, the alumina plate absorbs the near infrared light that is transmitted through the sample in order to prevent damage to the frame. The microscopy glass provides transparency to the near infrared wavelength and pressure on top of the samples. The deflection of glass is low, especially compared to that observed in PEEK films, thus providing even pressure to the samples. The toggle clamps provide a repeatable force to the glass plate to ensure a similar pressure of the sample. When the lever of the toggle clamp is depressed, the clamp mechanism reaches a singularity point, thereby maintaining the applied force. In addition, the toggle clamps allow for fast loading and unloading of samples. The applied force of the toggle clamp is approximately 50 N, resulting in an applied pressure of ~0.1 MPa.

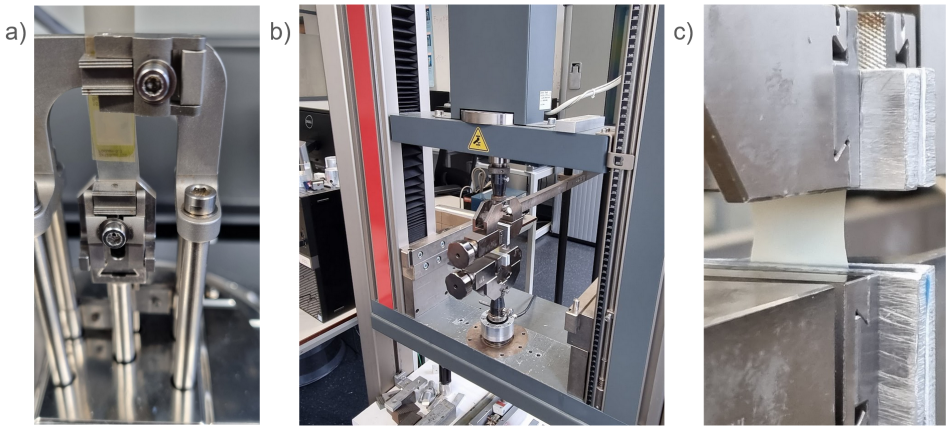

Figure 3.3: Overview of tensile testing equipment with a) close up of DMA Q800 tester, b) overview of Zwick Roell Z005 and c) close up of Zwick Roell Z005 clamping beaks.

3.2.4. Peel force tester

The Dynamic Mechanical Analyzer (DMA) Q800 is used for measuring the maximum peel force the welded samples can with stand. The testing apparatus has a range up to 18 N with a 10 µN resolution. The range of travel is 10 mm with a strain resolution of 1 nm. The samples will be clamped with a flat surface, as can be seen in figure 3.3 a. The samples will clamped as tight as possible to minimise the DMA has to pretension the sample.

3.2.5. Tensile tester

For larger required forces and travel the Zwick-Roell Z005 is required. This tensile tester is used for the tensile test of the heat treated samples discussed in subsection 3.3.2. Fine sandpaper is applied to the clamps to prevent slippage of the samples during testing.

3.2.6. Oven

The Memmert UN30 oven will be used for the thermal treatment test of single non-welded PEEK samples. The oven has a tolerance of 0.1 °C up to 99.9 °C and from 100 °C the tolerance is 0.5 °C. The oven has a temperature range from 40 to 300 °C.

3.2.7. Microscopes

Two different microscope (figure 3.4) will be used in this research, a reflecting light microscope and a transmission light microscope. The transmission light microscope, the Zeiss AxioScope A1, will be used to inspect the weld interface. The reflecting light microscope, the Keyence Digital Microscope VHX-6000, will be used to study the top surface, the roughness and topology of said surface, and to study the samples with polarised light.

3.3. Testing methods

3.3.1. Welding process

The research into the welding process consists of two phases. The first phase is to tryout to find out laser parameters at which two PEEK films can be lap welded. The literature on the laser transmission welding of PEEK films gives a direction in which to look, however, not a definitive answer. This is due to limitations with respect to the choice of laser. Where possible, the process variables were kept as similar as possible, such as in the type of absorptive coating. When a satisfactory weld recipe is found, the research will move into its second phase, parameter exploration. During parameter exploration all the parameters will be kept the same as the satisfactory weld recipe parameters and only one parameter will be varied to research its influence on the weld quality and strength.

a) 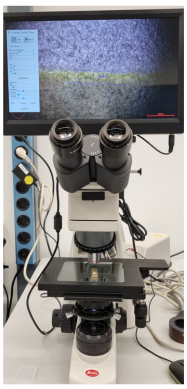 b)

Figure 3.4: The microscopes used in this project with a) the Zeiss AxioScope A1 and b) the Keyence VHX-6000

3.3.2. Thermal treatment test

Starting at room temperature (~25 ° C), the oven will be heated to 300 °C, with a step size of 25 °C. During each step, the samples will be placed in the oven for two minutes to ensure that the samples have reached the desired temperature and to accommodate the drop in temperature ~of 5 °C caused by opening the oven door. After the two-minute oven time, the samples will be air-quenched. Clearweld coated samples will be placed in the oven next to the heat treated samples. These samples will be used to study the effect of certain temperatures on the optical properties of the absorptive coating.

3.3.3. Data analysis

More than 150 samples will be used; therefore, it is crucial to implement a thorough way of handling the test data. Every welded and failed to weld sample will get specified name consisting of a letter corresponding to the test parameter and a number corresponding to the specific parameter value. Every parameter value will be used to weld four separate samples, unless it is clear beforehand that a certain parameter value will cause a burn or a non-weld. Of these four samples, the three most promising samples will be used for destructive testing.

4

Results

The results of the research into welding of PEEK films will be presented in this chapter. First, the spectral graph of PEEK and applied Clearweld coating will be shown. Secondly, the outcome of the thermal treatment test will be displayed. Lastly, the laser welding achievements will be presented.

4.1. Spectral properties PEEK and Clearweld

Spectral analyses was performed for determining the effectiveness of the Clearweld coating. The absorption, reflection, and transmission spectra of two 125 µm PEEK samples placed on top of each other, one with no layer, one with a single layer and the other with two layers of Clearweld coating, are illustrated in figure 4.1. The reflectance of Clearweld coated samples decreases considerably within the manufacturer-advised range optimised to 1100 nm. The absorptive coating effect is less prevalent at the transmissive spectra. A second layer of Clearweld decreases both the reflectance and the transmittance. The absorptive coating slightly increases the reflectance at wavelengths of 1300 and above. The amount of transmitted light has a larger increase and the crossing point with no applied Clearweld is at a lower wavelength. The portion of absorbed light increases substantially with a wavelength of 1100 nm and less. From 1250 nm onwards, the difference in absorption is significantly less. Around 1650 nm here is a peak in absorption and a coinciding drop in reflectance and transmittance. The smooth glossy side of PEEK has marginally more reflectance compared to the rough grainy side. The noisy signal on the left and right side of the graphs is due to a sensor sensitivity drop-off.

At the wavelength of 1030 nm, the absorbance unit is 1.17, 1.36 and 1.01 for single-, double sided and no Clearweld respectively. The percentage of reflectivity without Clearweld is 10.7 %, halving with one layer of coating to 4.8 % and almost halving again to 2.8 % with another extra layer. The transmissive spectra have a smaller change between samples with percentages of 10.0, 7.1 and 4.1 % in order of increasing number of Clearweld layers.

Discussion

The spectral properties measurements of the PEEK film and the PEEK film coated with the Clearweld adhesive reveal that the Clearweld coating reduces the reflective and transmissive properties of PEEK, thereby enhancing its absorption characteristics. This finding suggests that positioning the reflective sides of the PEEK at the welding interface, rather than externally, might be more advantageous. However, several limitations were noted in this study. Specifically, the reflective test only measured the 180° direct back-reflective light, which might not provide a comprehensive assessment. Interestingly, at higher wavelengths, particularly in the far-infrared spectrum, the Clearweld coating was observed to increase both the reflectance and transmittance of the PEEK film. This phenomenon lacks further research and a definitive explanation at this time.

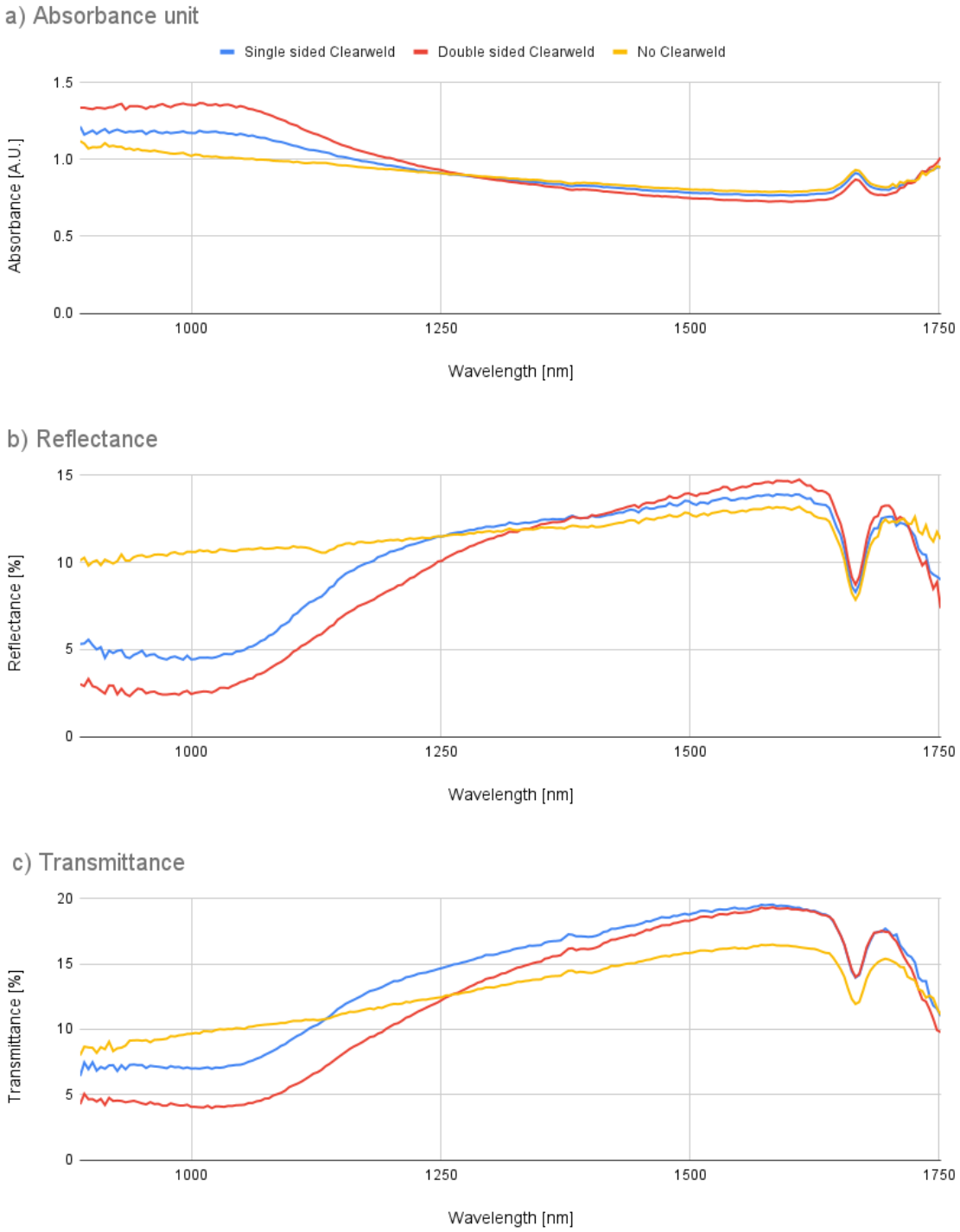

Figure 4.1: Spectral graphs of the a) absorbance, b) reflectance, and c) transmittance of two 125 µm PEEK films with no, single sided, and double sided Clearweld coating. The coating is applied to the smooth side of the PEEK films and the smooth sides are placed on top of each other. Single sided means only an applied Clearweld coating on one of the two films, double sided on both films

4.2. Thermal treatment

In this section, the outcomes of the thermal treatment test will be discussed. One issue encountered during this test was the drop in oven temperature when the oven door was opened. This temperature drop was approximately 5 °C. However, since the samples remained in the oven for 2 minutes, the temperature recovered to the intended level.

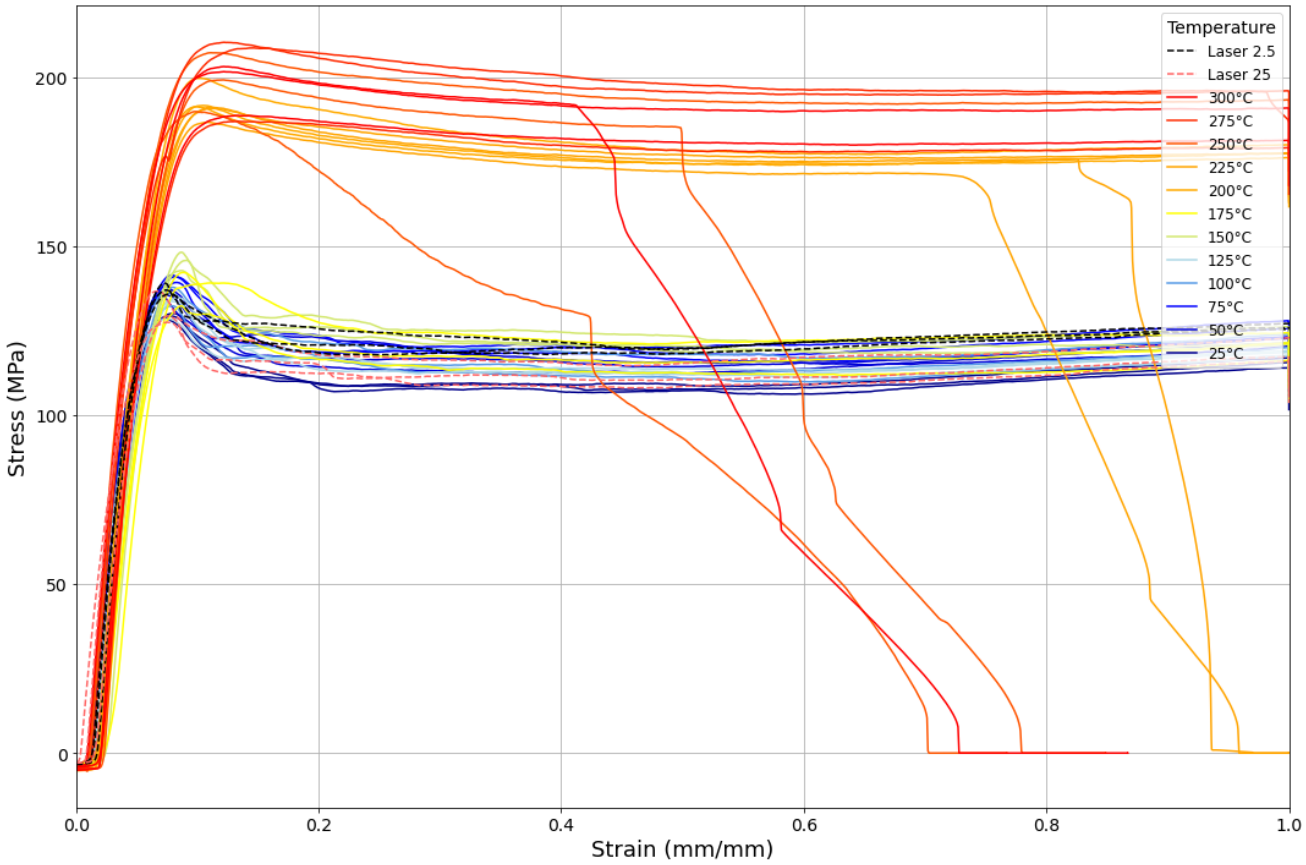

Figure 4.2: Stress strain relationship of PEEK thermal treated at the temperature range of 25 to 300 °C and treated with the 1030 nm laser. The dotted lines depict samples which were exposed to the 1030 nm laser with a speed of 2.5 and 25 mm/s.

4.2.1. Stress strain relationship

The non-temperature treated PEEK has a Young's modulus of 2.4 ± 0.4 GPa corresponding to the Young's modulus in table 3.1. The tensile stress of the samples treated around the glass transition temperature and below adhere to the value in the PEEK properties table 3.1. The temperature above the glass transition temperature, 150 and 175 °C, already rise a bit above the listed tensile stress. From 200 °C upwards there is a big jump in tensile stress to around 200 MPa. Furthermore, the shape of the graph changes during this jump from a clear summit to a ninety degree corner. At strain rates higher than 0.2 some 200 °C and higher samples already start to crack. In the stress-strain plots, the true strain is used due to the high deformations of the film (doubling in length).

The failure mode also showed an interesting side effect of change in material properties. At temperature treated PEEK of 200 °C and below all samples started necking, however they didn't fail when the elongation percentage of 100 was reached, meaning doubling in size. From 225 °C onwards some samples started showing cracks in the middle of the foil, some at the edge and one started cracking just above the clamp. These samples failed before the 100 % elongation was reached, with the red and yellow lines reaching the right side of the graph 4.2.

The 1030 nm laser-irradiated samples followed the same path as the lower temperature heat treated

samples. The samples where a higher laser speed (25 mm/s) was used reached a lower tensile strength compared to the lower speed (2.5 mm/s), indicating a greater amount of heat being irradiated into the sample.

4.2.2. Optical properties

In figure 4.3 the change of the optical properties of PEEK and the added Clearweld coating can be seen. There is no visible change in the first five samples, from the sample treated with room temperature (25 ° C) on the left to the second most on the right in the top row treated at 125 ° C. From the glass transition temperature upward, the samples curl up from their original flat state. The samples change from translucent to opaque. Although the Clearweld coating changes in appearance, it does not disappear, which it does when irradiated with 1030 nm laser light.

4.2.3. Roughness

The surface roughness and maximum height of the surface are plotted in figure 4.4. The measurements are taken on the rough side of the PEEK film. There is a slight decrease in height of the maximum surface feature with increasing temperature treatment. The average surface roughness does increase till just before the glass transition temperature, after that point the roughness decreases.

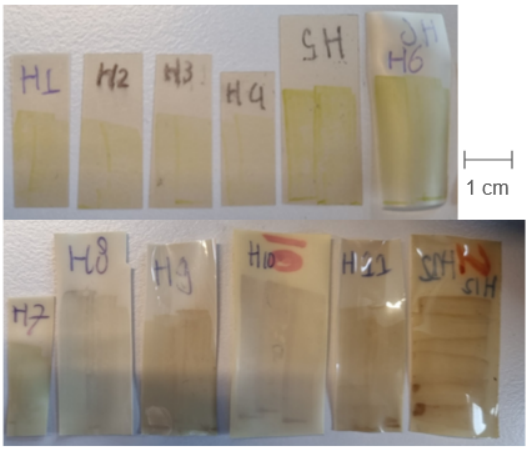

Figure 4.3: Thermal change in optical properties of PEEK with added Clearweld coating (From left to right, from top to bottom 25 °C to 300 °C with a step size of 25 °C)

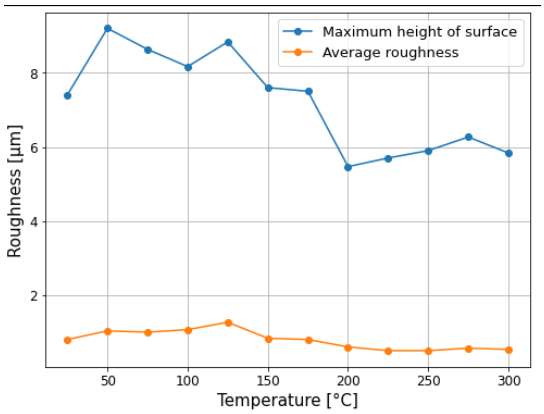

Figure 4.4: Average of maximum height of surface and average surface roughness of thermal treated samples for different temperatures

Discussion

Upon examination of the thermal treatment, several noteworthy observations emerge. First, two distinct groups of stress-strain curves can be identified. One group includes samples treated at 175 °C and below, along with the laser-treated samples. The other group comprises samples treated at 200 °C and above. The lower temperature-treated group (175 ° C and below) exhibits a more ductile behaviour, characterised by a curve with an initial peak, a slight decline, and a subsequent horizontal plateau. These samples did not show any signs of cracking, with some even enduring strain tests that extended beyond 100 % elongation, effectively doubling their original length. This prolonged horizontal path clearly indicates the ductility in the material.

The higher temperature-treated group (200 °C and above) displays a different pattern. Their stress-strain curves lack the initial peak, instead showing a sharp 90° angled corner, and samples in this group began to fail, exhibiting cracks. The elongation in these samples did not extend as far, indicating a more brittle material behaviour. Additionally, there is some variability in the graphs, which can be partly attributed to the deviation in sample lengths. With a ±1 mm deviation on a 20 mm sample length, this ±5 % variation causes a spread in the stress curves.

When examining the optical properties, notable changes begin to occur at the glass transition temperature of PEEK, which is just above 150 °C. At this temperature, the samples start to curl, transitioning from their initial flat state. Additionally, as the temperature increases, the samples become more opaque, whereas they were previously translucent. The Clearweld coating also undergoes noticeable changes starting from the glass transition temperature.

In terms of surface roughness, there is no significant change with higher temperature treatment. Although the feature size and average roughness decrease slightly after an initial increase up to 125 °C, the main structure of the rough, grainy surface remains largely unchanged.

The increase in strength and the decrease in ductility, along with the decrease in translucency and increase in opaqueness observed in the higher temperature-treated samples (between 175 °C and 200 °C), suggest that these changes are more likely related to the recrystallization temperature rather than the glass transition temperature. The recrystallization temperature lies just above this range and spans a wider range for PEEK. Therefore, the crystallinity of the samples is increased with thermal treatment. Interestingly, the laser-treated samples do not exhibit the same increase in crystallinity, suggesting that the laser treatment affects only the surface and not the bulk material. To accurately measure crystallinity, methods such as wide-angle X-ray scattering (WAXS) should be employed.

4.3. Welding

In this section the results optical inspection of the weld is shown.

4.3.1. Post-weld pictures

In figures 4.5 and 4.6, the left side shows images under normal light, while the right side shows images under polarized light. It is evident that polarized light provides much more insight into the actual phenomena occurring, as normal light images primarily show illuminated areas and air bubbles. Polarized light, on the other hand, reveals the structure of the patterns.

Specifically, in figure 4.5 b, with a welding speed of 10 mm/s, there is noticeable overlap between the welded laser lines in a vertical hatch orientation, corresponding to a pitch of 100 micrometers. In figure 4.6 b, the weld was only partially successful, with only half of the weld visible. This is likely due to a defect visible on the right side, where the lines intersect at an angle. The dark vertical spot on the left side indicates the weld, which is also observable in the image.

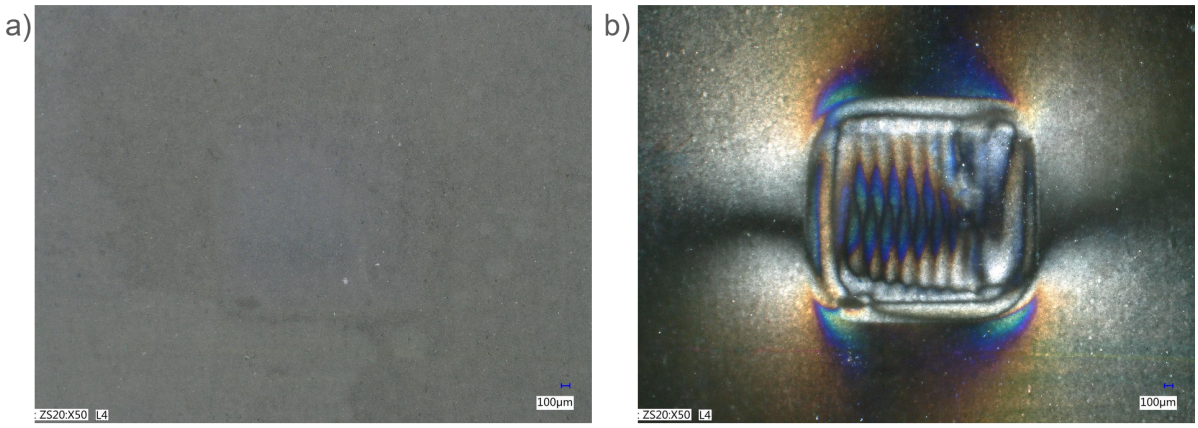

Figure 4.5: A microscopy picture of the weld with a speed of speed 10 mm/s at the same spot looked with a) normal and b) polarised light

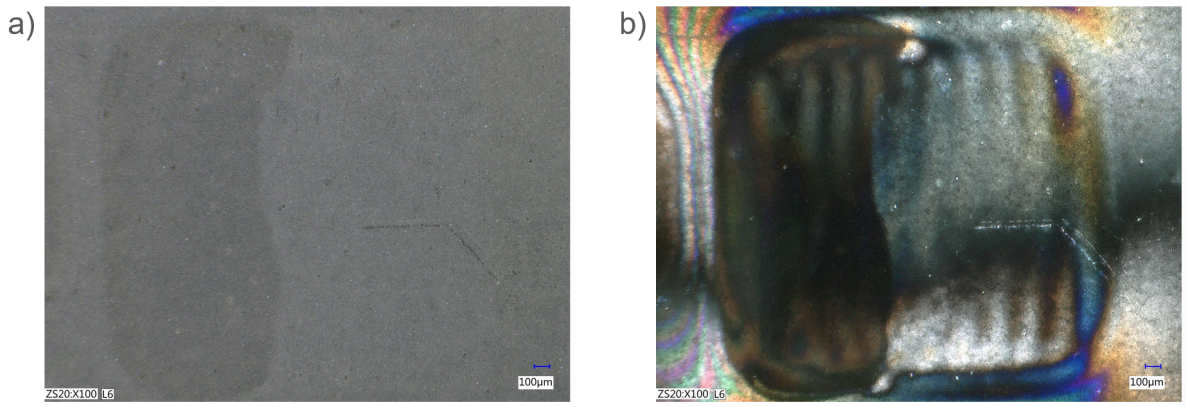

Figure 4.6: A microscopy picture of a half successful weld with a speed of speed 20 mm/s at the same spot looked with a) normal and b) polarised light

4.4. Peel tests

In this section, the results of the peel test will be presented, along with the geometrical changes that occurred during the peel test.

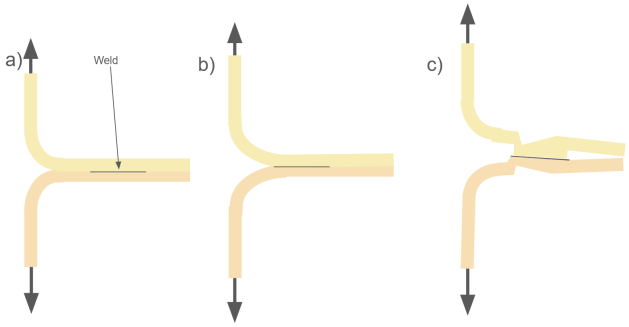

Figure 4.7: Different configurations of the welded PEEK films during T-peel tests

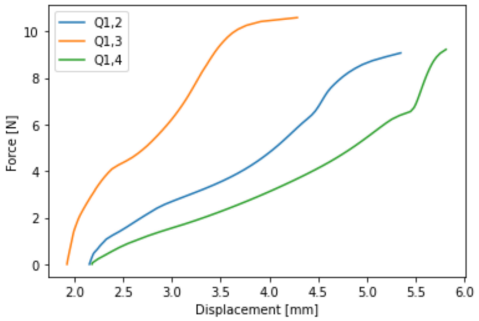

Figure 4.8: Force-travel curves for different horizontal hatch pattern samples

The T-peel test geometry for two welded films can be described in three distinct configurations based on how the films transition into the welded joint. These configurations can be seen in figure 4.7. In the first configuration (a), the films are welded together at a flat joint. The welded section is straight, and forces are applied to peel the films apart perpendicularly from the welded seam. The second configuration (b) modifies this setup by introducing a curved transition leading to the weld. This creates a smoother entry for the films, which can potentially reduce the stress concentration in the weld during the peeling process. In the third configuration (c), the films enter the weld at an angle, rather than a straight line or a smooth curve. This angled transition changes the stress distribution during the peel test and might simulate different peeling conditions compared to the other two configurations. These variations help in understanding how different shapes at the transition points influence the performance and strength of the welded joint under peeling forces.

In figure 4.8, the force-travel curves for a horizontal hatch pattern are shown. These curves represent three different samples, each with identical laser patterns, laser settings, and other parameters. However, it can be seen that they each follow a different path to ultimately reach roughly the same maximum peel force. This variation can be attributed to several factors. Firstly, the clamping position differs slightly by a few millimeters. Given that the samples are at most 30 mm in length, this difference accounts for a significant percentage. Additionally, as discussed in the previous paragraph, the samples undergo plastic deformation in different ways, particularly noticeable in the initial part of the graph. Ultimately, the focus of this research is on the maximum force achieved, rather than the specific path taken to reach it. The graph starts at a displacement of around 2 mm, this is the distance it took to

pretension the sample.

After the peel test, the weld area is plastically deformed as it has broken at the weld interface. The plastic deformation in the weld area can be seen in figure 4.9 a, which is a height map of the deformation. In figure 4.9 b, a cross-section of the deformation is shown. The right slope of the peak represents the area where the weld was located, with an angle of 20 degrees. It is evident that the plastic deformation of the peak is severe before the weld breaks at the weld interface.

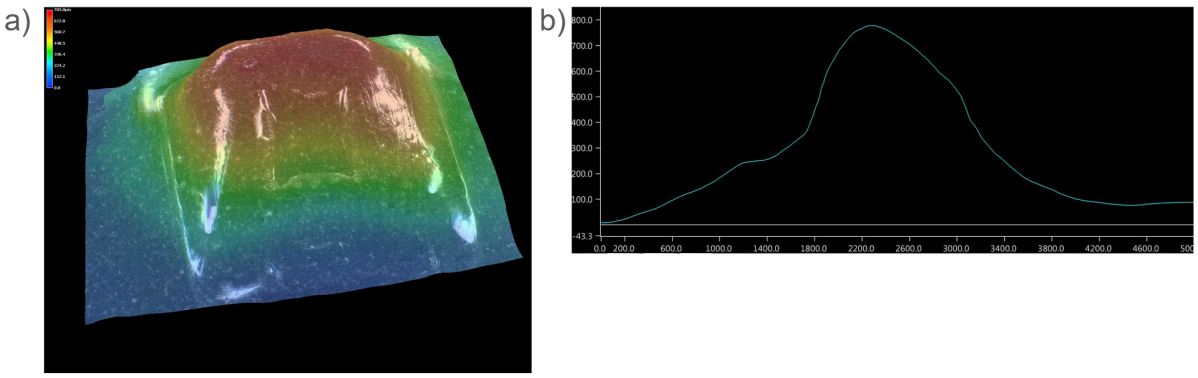

Figure 4.9: a) Profile of plastically deformation after peel test and at b) the angle of the slope at the right side of the top is 20° and the values are in µm

4.5. Laser parameters

In this section, the influences of the different laser parameters will be presented, along with images taken after welding. Additionally, fluence calculations will be shown with respect to the pitch size and laser speed.

4.5.1. Fluence calculations

The Pharos laser source provides the energy of a single laser pulse. The fluence can be calculated with this energy, the path length of the laser, the total area, and laser parameters like the burst duration, pulse rate, and burst rate (see figure 2.2). The calculation can be found below:

$$Pulses\ per\ Burst\ =\ Burst\ Duration\ \times Pulse\ Rate\ \rightarrow\ 100\ \mu s \times 157,000\ Hz\ = 15.7$$

The pulses per burst will be rounded down because the number of pulses must be an integer.

$$Total\ Pulses\ per\ Second\ =\ Pulses\ per\ Burst \times Bursts\ Rate\ \rightarrow\ 15 \times 100\ Hz\ =\ 1500$$

The pulse rate, burst rate, and burst duration are kept constant throughout all experiments. The path length and the laser speed change with different tests. Changing these will provide different fluence values. This calculation will be performed with standard values of a speed of 25 mm/s and a pitch of 100 µm. A square area of 2 by 2 millimetres and filled with lines with a pitch of 100 µm, will have 21 lines with a length of 2 mm and a total path length of 42 mm. The time it takes for the laser with a speed of 25 mm/s to complete the path is 1.68 seconds.

$$Total\ Energy\ =\ Pulses\ per\ Second \times Total\ Seconds \times Energy\ of\ a\ Pulse\ \rightarrow\ 1500 \times 1.68\ s \times 13.7\ \mu J\ = 0.0345\ J$$

To calculate the fluence, the total energy irradiated by the laser has to be divided by the irradiated area.

$$Fluence\ =\ 0.0345\ J\ \div\ 4\ mm^2\ =\ 0.008631\ J/mm^2$$

In table 4.1 the fluence values for different pitch sizes are shown. In table 4.2 the different laser speeds are shown with the corresponding fluence values. With doubling either the pitch size or the speed the fluence is almost halved.

Table 4.1: Fluence values for different pitch sizes

Pitch Size (µm)	Fluence (J/mm^2)
25	0.034524
50	0.017262
100	0.008631
150	0.005754
200	0.004316
400	0.002158
500	0.001726

Table 4.2: Fluence values for different speeds with a pitch of 100 µm

Speed (mm/s)	Fluence (J/mm^2)
2.5	0.08631
5	0.043155
7.5	0.02877
10	0.0215775
15	0.014385
20	0.01078875
25	0.008631
30	0.0071925
35	0.00616643
40	0.00539375
50	0.0043155
60	0.00358792
70	0.00308893
90	0.00239194

Discussion

The fluence ($0.008631\ J/mm^2$) is rather low in comparison to other welding methods. The reason is that only the weld interface has to be heated, not the bulk material. The laser ray does not first have to melt it's way down through the top material. The linearly decreasing peel force strength in the laser speed figure 4.10 can be correlated to the linearly decreasing fluence with higher speeds, as seen in table 4.2. There is a threshold where the fluence becomes too high. This threshold is in the area of laser speeds of 7.5 and 10 mm/s corresponding to fluences of 0.0288 & $0.0216\ J/mm^2$ respectively. As with lower speeds and thus higher fluences, the formation of bubbles at the surface has occurred. A more evenly distributed beam profile (high M^2 factor) is beneficial due to the more evenly spread energy density. Also the tail of the curve is smaller thus influencing the side less.

4.5.2. Laser speed

In graph 4.10, the maximum force and fluence are shown as functions of laser speed. Initially, as speed increases, fluence decreases. This reduction in fluence affects the maximum force. At speeds below 10 mm per second, excessive fluence results in poor weld performance, indicating a maximum fluence of roughly 0.02 to 0.03 J/mm^2. The highest maximum peel force is observed between approximately 10 and 15 mm/s. Beyond this range, as the laser speed continues to increase, the maximum force decreases, exhibiting a semi-linearity.

4.6. Defocussing distance

In the defocussing versus maximum peel force graph 4.11, the defocussing distance is compared to the maximum peel force at intervals of 1 mm. The samples were burnt at defocussing distances of 0, 1, 2 and 3 mm. At 0 mm, no weld was formed, which is why it does not appear on the graph. Starting from a defocussing distance of 1 mm welds did form. An increasing weld strength is observed at smaller defocussing distances of 1, 2, and 3 mm, reaching a peak around 5 to 6 mm. Beyond 7 mm of defocussing distance, the maximum peel force decreases again.

Defocussing line width

In figure 4.12, the line width of various lines is depicted through a transmission microscope. The number on the top left of each image indicates the defocussing distance used. At 2 mm or less of defocussing distance, a clear burning of the entire peak at the centre point is observed. Between 3 to 4 mm of defocussing distance, the burn spots decrease significantly and appear more as a spread of several points. In addition, the clear weld area, indicated by the yellow region, is more dispersed than the black dots. At 5 mm of defocussing distance and above, burning spots are no longer present, and good welding spots are visible, each with its own distinct features.

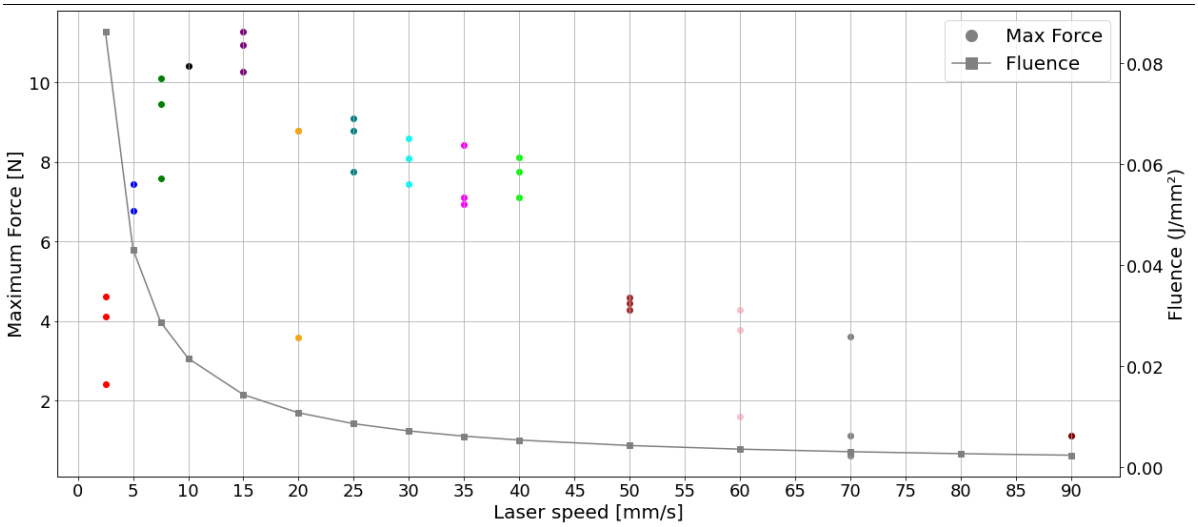

Figure 4.10: Peel force at different laser speeds and the fluence (table 4.2) corresponding to the speed

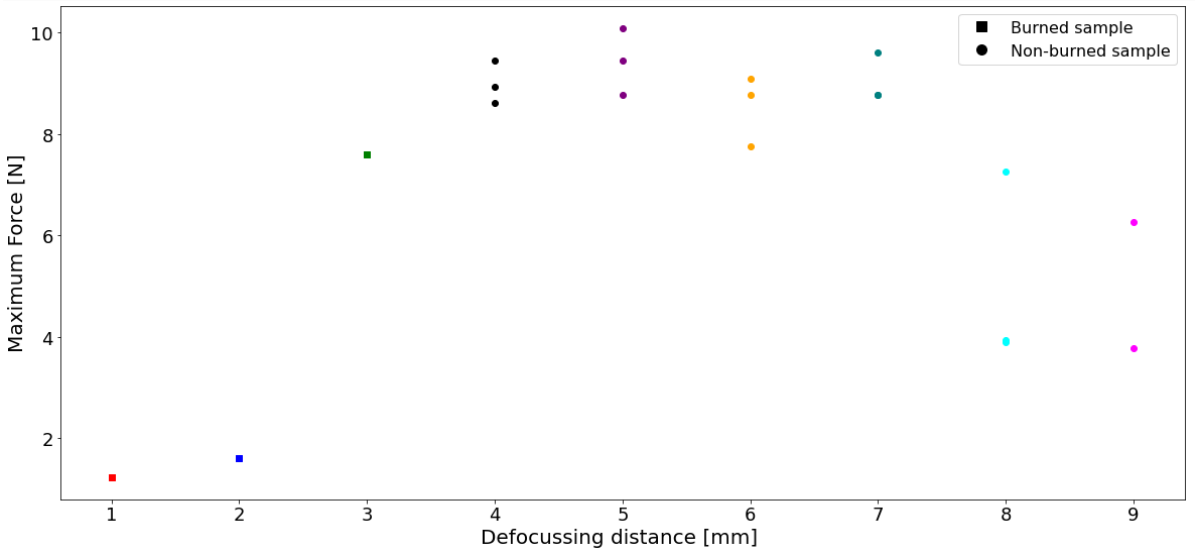

Figure 4.11: Maximum peel force for different defocussing distances

In graph 4.13, the line width compared to the focusing distance is shown. The line width is measured with polarised features as seen in the appendix [appendix will be added later]. A quadratic fit is applied over the data points. It can be observed that the line width starts at 0 at the smallest focal feature size of the laser used, which is 30 µm. The line width then increases rapidly, reaching its highest point at a focusing distance of 6 millimeters. After this peak, the graph shows a decline indicating a decrease in fluence. The maximum line width is approximately 400 µm.

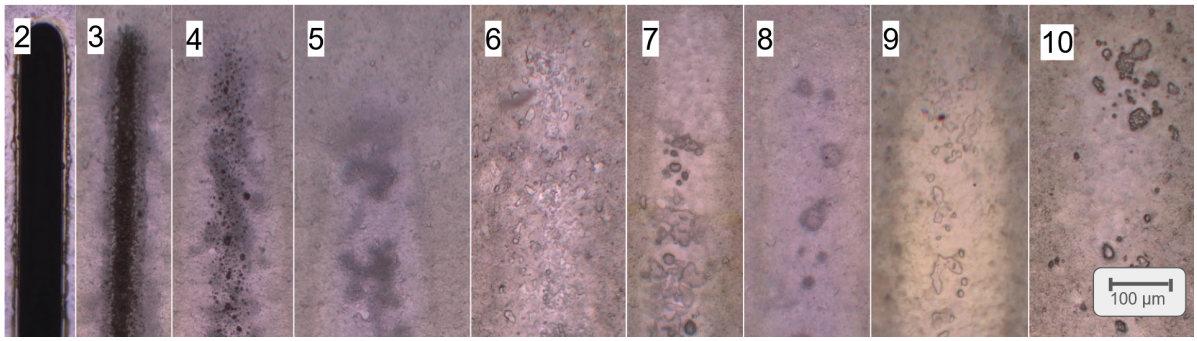

Figure 4.12: transmission-microscope-single-line

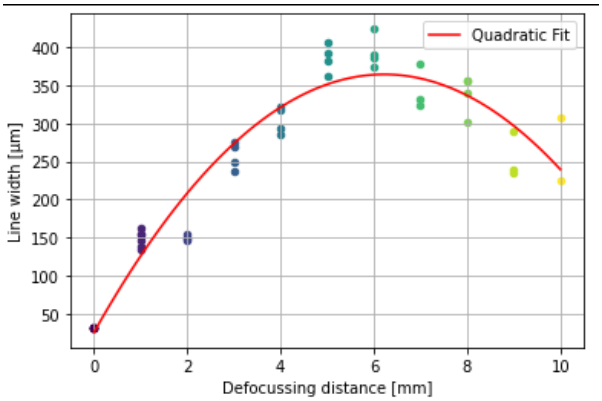

Figure 4.13: The line width of different defocussing distances. The formula of the quadratic fit is $y = -8.75x^2 + 108.90x + 25.48$

Discussion

The defocussing line width exhibited interesting effects. Initially, the line width increased with larger defocussing heights but then started to decrease again. This phenomenon is likely related to the energy density distribution, as illustrated in chapter 2. At low defocussing depths, the energy density is very high at the beam's center. As the beam spreads more, the energy density becomes more evenly distributed before eventually dropping, as can be seen in figure 2.3 a. For optimal welds, an even non-Gaussian beam profile is desirable, effectively leading to a M^2 factor approaching infinity. Additionally, burning stops between 4 and 5 mm of defocussing depth, indicating a threshold where the energy density falls below the flammability or burning point of the polymer. The Clearweld coating appears more sensitive, as evidenced by the greater disappearance of the green Clearweld under the laser, visible through optical microscopy.

4.7. Weld shape

In this section, the influence of various weld patterns and shapes on weld quality will be examined. Initially, the pitch distance will be analysed. Subsequently, the performance differences among various hatch patterns will be explored.

4.7.1. Pitch distance

In figure 4.14, it is demonstrated that the pitch distance has a significant influence on the shape of the weld when examined under polarised light. It is evident how the pitch distances of 25 and 50 µm maintain a uniform block. From 100 µm onwards, the structure changes incrementally until around 400 µm where the pitch lines still overlap. At 500 µm, spaces begin to appear between the pitch lines. The up and down movement of the laser is also observed in pitch sizes ranging from 100 to 500 µm. It can be seen that the lines exhibit a tapered form. Moreover, one will observe fringes around the edges when

viewed under polarised light. Additionally, at the lowest pitch size values, it can be observed that bubbles have formed. An indication of bubble formation is the vaporisation of the Clearweld coating. The outer edges of the square weld area are progressively diminishing and becoming less sharply defined with larger pitch sizes.

In figure 4.15, the maximum weld force is plotted for various pitch sizes, the graph also shows the fluence with respect to the pitch size as presented in table 4.1. In the graph there are three distinctive areas, illustrating a clear relationship between fluence and maximum peel force. In the leftmost part of the graph, with pitch sizes of 25 µm, the maximum fluence threshold is crossed, indicating an excessive amount of energy irradiated to the PEEK film. In the second area, the weld force is at a maximum between 50 and 150 µm. Starting from 200 µm and extending up to 500 µm, a decreasing fluence can be observed, the maximum force follows this trend.

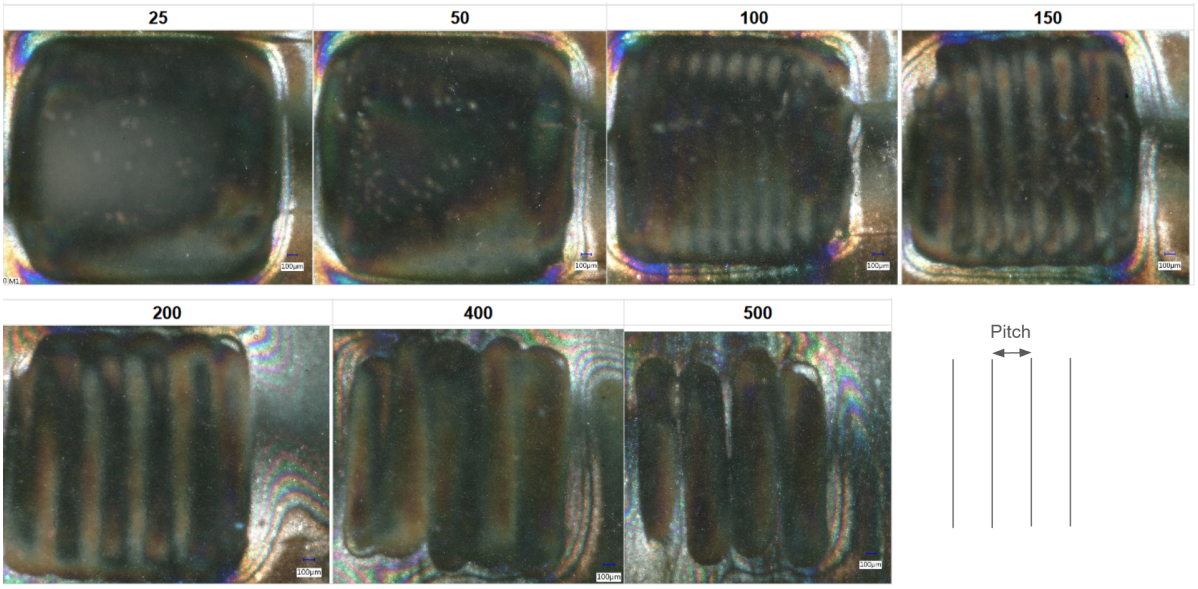

Figure 4.14: Overview of different pitch distances in polarised light(Pitch in µm)

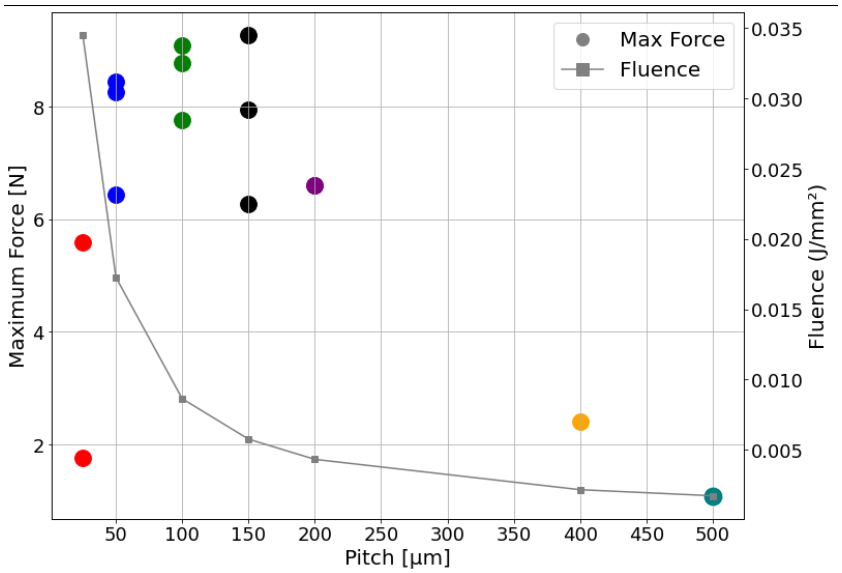

Figure 4.15: The max peel force of different pitch sizes and the fluence at the respective pitch sizes are shown

4.7.2. Hatch pattern

In figure 4.16, different hatch patterns are displayed, and the resulting maximum peel force for each pattern. The horizontal, vertical and diagonal orientations of the hatch have the highest peel force at around 10 N. There is a slight decrease in force when an outline is added to the hatch patterns, which can be seen in the erode of the pattern and at the other hatch patterns with outline. For the erode pattern, the middle portion of the square is not welded. The spread of the maximum peel force is larger in the erode pattern and the hatch patterns with outlines.

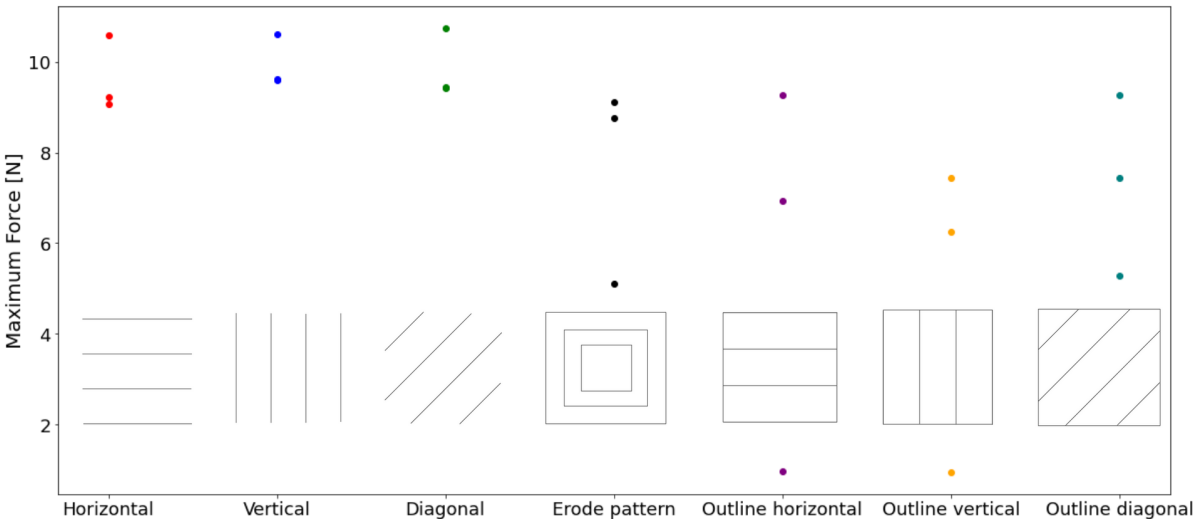

Figure 4.16: Maximum peel force for different hatch patterns

4.8. Welding different thicknesses

Different material thicknesses, both individually and in combination, are examined in figure 4.17. The study explores various combinations of the same and different thicknesses. It is clearly evident from the figure that the welding process is optimised for joining two films each of 125 µm. There is a noticeable decrease in the maximum peel force with decreasing overall thickness. There is no substantial difference in weld strength, whether thicker films are placed on top before welding, or vice versa.

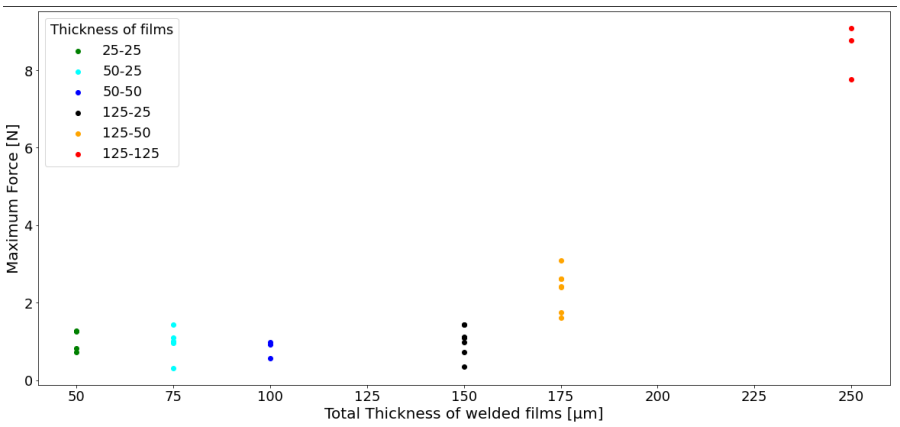

Figure 4.17: The maximum peel force for different film thickness combinations

Discussion

The peel test revealed that even slight changes in clamping could influence the sample's movement. With a clamp stroke of only 2 to 3 cm, minor adjustments affected the deformation of the film more than the weld itself. Around the weld edges, during the second phase of the test, the film began to deform,

indicating stress concentration points. All peel test samples broke at the weld edge, highlighting the weld's vulnerability to applied torque. In tensile tests, the welds demonstrated considerable strength. All samples exhibited necking and did not break at or near the weld interface, showing yield strengths comparable to that of PEEK itself. This indicates that while the welds are robust in terms of tensile strength, they are more susceptible to failure under peel stresses.

The difference in different thicknesses in the defocussing distance, as the total thickness difference is at maximum 20 % of the step size of the defocussing plot. The hatch distance does not significantly influence the weld quality, nor does the hatch pattern, although an outline slightly decreases the maximum force. This report does not provide an explanation for these observations, suggesting that more research is needed to understand the underlying mechanisms and potential effects in future applications.

Polarized light microscopy reveals significantly more information compared to normal light microscopy. It clearly shows the laser path direction and the hatch sizes, providing a wealth of detail about the welding process and the resulting structure. This method enhances the ability to analyze the precise effects and quality of the welds.

4.9. Welding thermoformed sheets

In figure 4.18 a side view of the welds with different top flat layer thicknesses is shown. It can be seen that with a thinner material, the film follows the contour of the 3D thermoformed material better. To achieve a successful weld, the 3D features required support from a resin-printed positive mold, as can be seen in Appendix A figure A.2. Attempts to weld without such supporting features resulted in sub optimal weld quality, with the 3D features deforming slightly and reverting towards their original flat state.

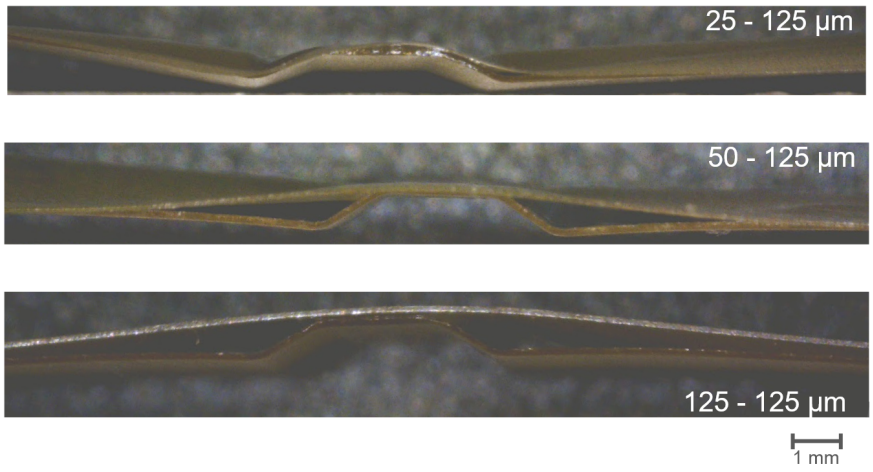

Figure 4.18: Side views of thermoformed welds with different top layer thicknesses welded to a thermoformed 125 µm PEEK film. From top to bottom picture with thicknesses of 25, 50 and 125 µm.

5

Discussion & Conclusion

5.1. Discussion

During the welding process, several improvements could be made. Dust particles and hairs were still visible at the weld interface, causing no-weld areas due to the lack of contact between the PEEK interfaces. This significantly reduces the strength of the weld. It is crucial to minimize these particles, which was not fully achieved as the laser was situated in a non-cleanroom environment, though mitigation efforts were made. Further research is needed on the optimal application of the Clearweld coating. When there were doubts about the application of the coating, a double coating was used, but its effectiveness has not been thoroughly tested.

The toggle clamps applied relatively low pressure compared to other welding methods for plastics, such as using pressures of several megapascals. Although higher forces were tested and the welds showed optical improvement, their strength was not evaluated. Future studies should investigate this aspect. The weld pressure was evenly distributed through the microscope glass, which exhibited slight bending. This could be improved by using thicker glass or redesigning the clamp to apply more uniform pressure.

Handling thinner PEEK films (25 or 50 microns) often resulted in wrinkles and local plastic deformation, which negatively impacted weld formation and strength. The welding process should be optimized for different thicknesses of PEEK films in future research to address these issues. For 3D welds, the support structure of the positive mold was essential. Without it, the structure of the freshly thermoformed samples deformed excessively, leading to poorer weld quality due to the uneven surface interface of the two pre-welded films. While different thicknesses could be welded together in 3D welds, the overall weld strength has not been thoroughly evaluated and there is room for improvement.

5.2. Conclusion

Based on the results of this report the following conclusions were made:

1. Laser transmission welding is a proficient way of joining thermo formed sheets for the MECOMOS manufacturing method.
2. Laser transmission welding is able to weld thin films of different thicknesses together.
3. Optimal parameters for welding 125 µm thick PEEK films together is a speed between 10 and 15 mm/s, a defocussing distance between 4 and 7 mm, and a pitch distance between 50 and 150 µm.
4. It is a challenge to maintain the shape of the material while welding. Laser transmission welding does heat the material locally above the melting temperature.
5. Fluence wise there is an optimal point just below a threshold, this threshold lies between a fluence of 0.03 and 0.02 J/mm^2.

5.3. Recommendations and future work

To perform a successful PEEK laser transmission weld, the following recommendations are useful to implement:

1. Make sure to eliminate dust particles to make sure the PEEK films are touching each other.
2. Make sure the pressure at the weld area is applied evenly.
3. Make sure the Clearweld coating is evenly spread, it is better to have too much than too little coating.
4. The handling of films with thicknesses of tens of micrometres should be done with care to minimise the amount of wrinkles in the film.

There are interesting research directions which could be pursued in the future:

1. Improving the weld parameters for thinner films and for welding different thicknesses.
2. Design to improve the pressure application of 3D welds.

References

[1] Jasmin Althaus et al. “Anisotropy in polyetheretherketone films”. In: *Journal of Nanophotonics* 6.1 (2012), pp. 063510–063510.

[2] Negin Amanat et al. “Transmission laser welding of amorphous and semi-crystalline poly-ether–ether–ketone for applications in the medical device industry”. In: *Materials & design* 31.10 (2010), pp. 4823–4830.

[3] *APTIV Films 1000 data sheet*. Oct. 2023.

[4] F Becker and H Potente. “A step towards understanding the heating phase of laser transmission welding in polymers”. In: *Polymer Engineering & Science* 42.2 (2002), pp. 365–374.

[5] Mridusmita Roy Choudhury and Kishore Debnath. “Current and future trends in micro-joining and nano-joining”. In: *Joining Processes for Dissimilar and Advanced Materials* (2022), pp. 209–239.

[6] Clearweld. *CLEARWELD 900 SERIES*.

[7] Ward Dijkman. *Joining methods at the microscale (TU Delft internal literature report)*. 2023.

[8] Claus Emmelmann and Juan Pablo Calderón Urbina. “Analysis of the influence of burst-mode laser ablation by modern quality tools”. In: *Physics Procedia* 12 (2011), pp. 172–181.

[9] Luis FFF Gonçalves et al. “Laser welding of thermoplastics: An overview on lasers, materials, processes and quality”. In: *Infrared Physics & Technology* 119 (2021), p. 103931.

[10] Yousuke Kawahito et al. “Relationship between melt flows based on three-dimensional X-ray transmission in situ observation and spatter reduction by angle of incidence and defocussing distance in high-power laser welding of stainless steel”. In: *Welding International* 32.7 (2018), pp. 485–496.

[11] Rolf Klein. *Laser welding of plastics: materials, processes and industrial applications*. John Wiley & Sons, 2012.

[12] Rakesh Kumar et al. “Overview on metamaterial: History, types and applications”. In: *Materials Today: Proceedings* 56 (2022), pp. 3016–3024.

[13] Steven M Kurtz. “An overview of PEEK biomaterials”. In: *PEEK biomaterials handbook* (2012), pp. 1–7.

[14] Yuxuan Liu et al. “Study on microstructures and mechanical performance of laser transmission welding of poly-ether-ether-ketone (PEEK) and carbon fiber reinforced PEEK (CFR-PEEK)”. In: *Journal of Laser Applications* 34.4 (2022).

[15] *Mechanical metamaterials for compact motion systems (MECOMOS) project website*. URL: `https://www.tudelft.nl/3me/over/afdelingen/precision-and-microsystems-engineering-pme/research/mechatronic-system-design-msd/msd-research-mechanical-metamaterials-for-compact-motion-systems-mecomos`.

[16] *Pharos Femtosecond laser data sheet*. 2018.

[17] Richard S Quimby. *Photonics and lasers: an introduction*. John Wiley & Sons, 2006.

[18] Gian-Luca Roth, Stefan Rung, and Ralf Hellmann. “Welding of transparent polymers using femtosecond laser”. In: *Applied Physics A* 122.2 (2016), p. 86.

[19] Renjie Tian et al. “Experimental study and numerical simulation for the interaction between laser and PEEK with different crystallinity”. In: *High Performance Polymers* 33.8 (2021), pp. 851–861.

[20] AK Van der Vegt. *From polymers to plastics*. VSSD Delft, 2006.

A

Appendix A - LTW step by step guide

In this appendix, a step-by-step guide of the welding process used in this research will be shown.

0. Clean the PEEK surface with Isopropanol
    i. Wear latex gloves when handling Isopropanol
1. Apply the Clearweld coating to both interface surfaces (figure A.1)
    i. Apply the coating in a fume hood and let the acetone vaporise for at least 10 seconds
    ii. Apply the coating on the smooth side of the PEEK film
2. Place the coated surfaces on top of each other
    i. Try to eliminate dust as much as possible by doing the placing in a low dust environment
3. Apply pressure by closing the clamps (figure A.2)
    i. Place and align the samples on the alumina plate
        A. In case of 3D welding, place a support underneath the sample
    ii. Place a microscopy glass on top of the PEEK films
    iii. Close the toggle clamps
4. Focus the laser and start welding (figure A.3)
    i. Focus the laser on the PEEK film
    ii. Add the defocussing distance to the vertical position start point
    iii. Set the start point of the weld
    iv. Start welding

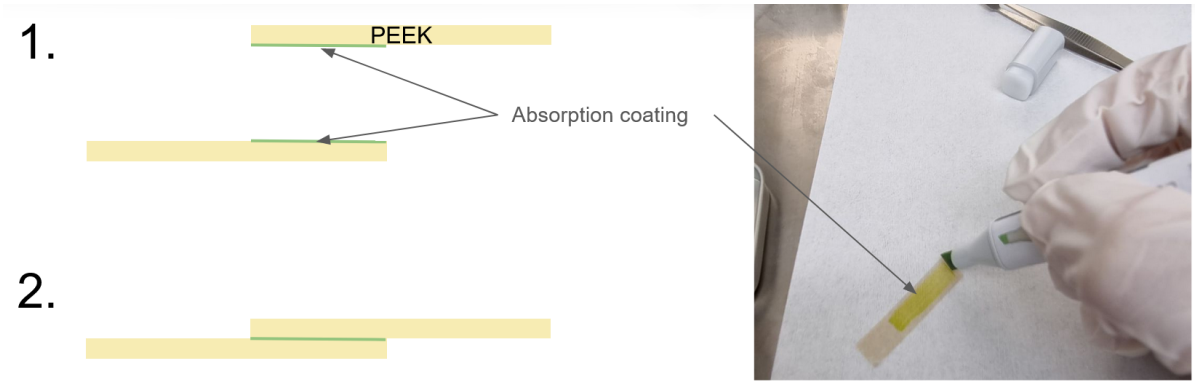

Figure A.1: Step 1, applying the Clearweld coating to both interface surfaces, and step 2, placing the coated surfaces on top of each other

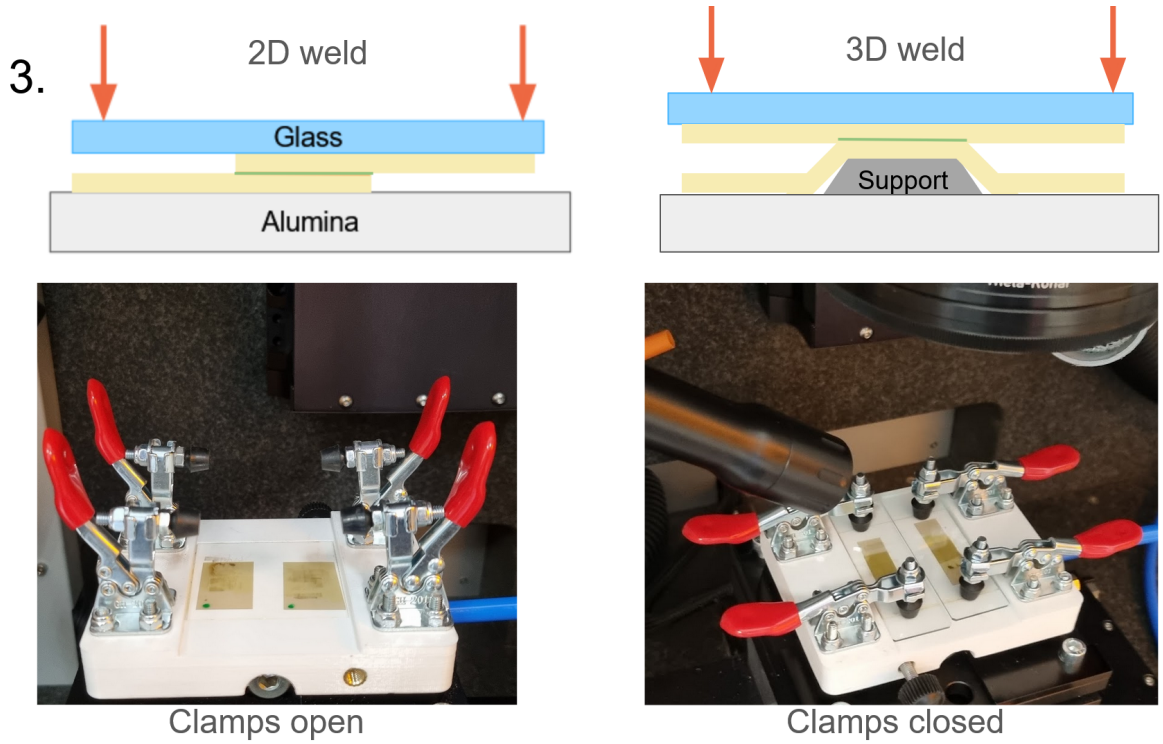

Figure A.2: Step 3, closing the clamps

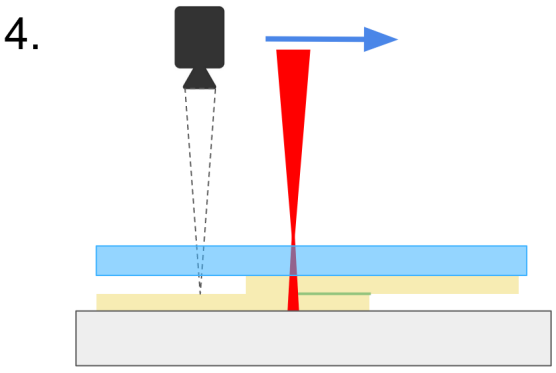

Figure A.3: Step 4, focus the camera on the weld interface and start the laser welding

A.1. Laser parameters

In table A.1 the optimal welding parameters for lap welding 125 µm thick PEEK films with Clearweld absorptive coating are shown.

Table A.1: Optimal welding parameters for lap welding 125 µm thick PEEK films with Clearweld absorptive coating

Laser parameters		
Speed	15	[mm/s]
Jump speed	2000	[mm/s]
Burst Rate	100	[Hz]
Burst Time	100	[µs]
Repetitions	0	[#]
Pulse rate	157000	[Hz]
Power	100	[%]
Defocussing distance	6	[mm]
Pitch	100	[µm]
Pulse energy	13.7	[µJ]
Laser frequency	1100	[kHz]